1948

Plastic behavior of wide-flange beams, Welding Journal, Vol. 27, p. 583-s, Nov. 1948, Reprint No. 63 (48-2)

W. W. Luxion

B. G. Johnston

Plastic Behavior of Wide Flange Beams

by

W. William Huxion
and
Bruce G. Johnston

Progress Report No. 1: Welded Continuous Frames and Components

Plastic Behavior of Wide Flange Beams

This report presents results of wide flange sections tested as simple beams with third point loading through the elastic and into the plastic range

by W. William Luxion and Bruce G. Johnston

THE Welding Research Council, through its Structural Steel Committee, directed in December of 1945 that the resumption of its work at Lehigh University should be on the subject of fully continuous welded frame construction. Prior to interruption by the war, a number of projects at Fritz Laboratory had been sponsored on flexible beam-to-column building connections and the possibilities of the "semi-rigid" connections also had been explored.

In suggesting the new program it was thought that the advantages of welding could best be realized if the fully continuous type of construction were used, thereby leading to the greatest ultimate or collapse strength of the structure. The work was to commence with simple beam tests of wide flange sections and lead to tests of continuous beams, welded connections and welded continuous frames. In Great Britain, J. F. Baker and his associates have had under way a similar investigation, utilizing tests of small models, the results of which have been presented in a number of reports of the British Welding Research Association.

In 1946 the American Institute of Steel Construction also resumed sponsorship of research at Fritz Engineering Laboratory, continuing its prewar investigation of steel columns. Emphasis was placed on the behavior of the column as part of a continuous frame. This naturally led to the suggestion, in 1947, to unite the W. R. C. and A.I.S.C. work under a single coordinated program. This move was later approved by the Structural Steel Committee which also expedited the work by increasing the allotted annual budget. The Bureau of Yards and Docks and the Bureau of Ships of the U. S. Navy, through the Office of Naval Research, undertook the sponsorship of specific features of the over-all program. The American Iron and Steel Institute added their financial support, and, at the time of writing this report, all phases of the work are now underway.

Acknowledgment is due William Spraragen, director of the Welding Research Council; LaMotte Grover, chairman of the Structural Steel Committee and T. R. Higgins, chairman of the Lehigh Project Subcommittee for their continued guidance and assistance. A. Amirikian, of the Bureau of Yards and Docks, was also particularly helpful in providing the initial impetus to the work and advising as to its detailed direction.

W. William Luxion was formerly Welding Research Council Fellow at Fritz Engineering Laboratory, now with Roberts and Schaefer Engineering Co., Chicago, Ill. Bruce G. Johnston is director of Fritz Engineering Laboratory and Professor of Civil Engineering, Lehigh University, Bethlehem, Pa.

Paper presented at the Twenty-ninth Annual Meeting, A. W. S., Philadelphia, Pa., week of Oct. 24, 1948.

INTRODUCTION

This report presents results of wide flange sections tested as simple beams. Third point loading was used to provide a central section wherein pure moment without shear would be obtained and the basic bending behavior at initial yielding and in the plastic range could be studied. An extensive exploration of elastic and plastic strains was made throughout each of the beams in the regular test series.

The tests reported on herein were as follows:

Pilot Test No. 1	8WF31	as-delivered	12 ft. 0 in. span
Pilot Test No. 2	8WF40	as-delivered	12 ft. 0 in. span
Regular Test No. 1	8WF40	as-delivered	14 ft. 0 in. span
Regular Test No. 2	8WF40	annealed	14 ft. 0 in. span
Regular Test No. 3	8WF67	as-delivered	14 ft. 0 in. span
Regular Test No. 4	8WF67	annealed	14 ft. 0 in. span

The bending behavior at a particular location along a beam may be depicted by means of an "M-ϕ" graph, in which the moment, M, is the ordinate, and ϕ, plotted as the abscissa, is the rate of change of slope of the beam axis at the point in question. ϕ is inversely proportional to the radius of curvature of the beam axis, $\phi = 1/R$. Within the elastic range, the bending moment is proportional to the curvature and the M-ϕ curve is a straight line, the elastic constant of proportionality being equal to EI.[1]

$$M = EI\phi \qquad (1)$$

If the bending moment is constant over any length of the beam, as in the central third of the test beams, ϕ is also constant within this region and the beam bends into a circular arc. Within this section ϕ may be determined by deflection readings at three different locations along the beam.

Some of the factors influencing the bending behavior will be discussed herein under the following headings: (1) stress-strain properties of structural steel; (2) shape of cross section; (3) local buckling, (4) residual stresses.

Stress-Strain Properties of Structural Steel

The well-known tensile stress-strain properties of structural steel are illustrated in Fig. 1 (*a*). A proportional limit, not shown, is usually observed somewhat below the upper yield point. The upper yield point represents a condition of instability, affected by rate of loading, surface condition and other factors. The lower yield point is the more stable and well defined of the two, being the nearly constant stress at which continued slow average strain rate is maintained, while zones of yielded material spread from their points of inception. The total plastic strain during the constant lower yield point stress is usually 10 to 20 times as large as the initial elastic strain (Fig. 1 (*a*)). The yielded regions finally become more or less general, the material starts to strain-harden, and the stress increases.

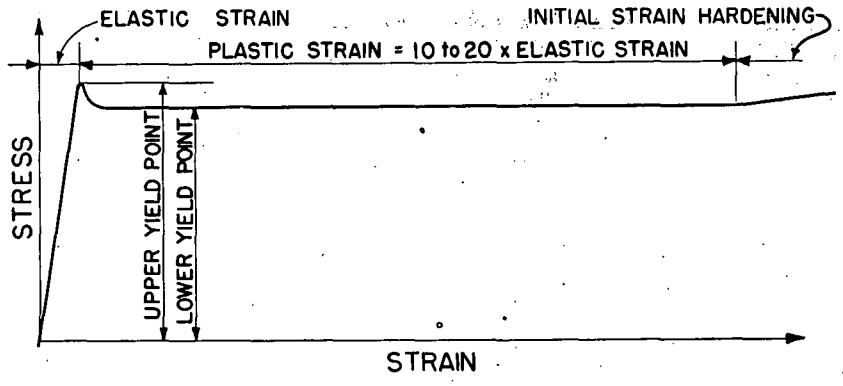

FIG. 1a . TYPICAL SHAPE OF STRESS–STRAIN DIAGRAM FOR STRUCTURAL STEEL.

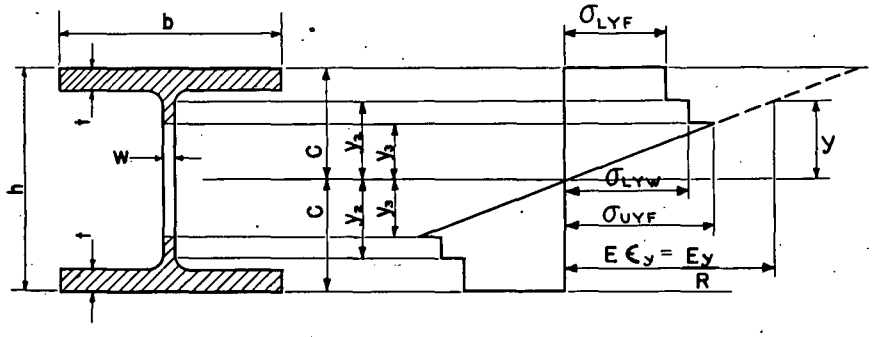

FIG. 1b ASSUMED STRESS DISTRIBUTION IN STEEL BEAM STRAINED BEYOND ELASTIC RANGE.

One of the objects of these tests was to compare experimental M-ϕ curves with those calculated from the tensile and compressive stress-strain diagrams of the same material. General procedures for calculating M-ϕ curves for any shape section from any given stress-strain data, or the reverse, have long been available.[2,3] These procedures assume* that the longitudinal strain in the elastic, plastic and intermediate stages of bending varies linearly across the beam section and that the strain in the most stressed fiber is uniformly the same along any region of constant moment at all stages of yielding. These conditions may be approximately realized in the case of most nonferrous alloys as well as some ferrous materials that have a continuously increasing stress-strain curve. In the case of structural steel, yielding commences intermittently along the most stressed fibers and proceeds downward in localized planes into less stressed regions, as well as along the beam. An extensive investigation of this process has recently been reported by the University of Illinois.[4] The "theoretical" curves reported herein are nevertheless based on the usual assumption of uniform yielding. It will also be assumed, as is commonly the case, that the web material has a different yield point than the flange.

Calculation of a theoretical M-ϕ curve is extremely simple if the stress-strain curve is as shown in Fig. 1 (a) and is assumed the same in tension as in compression. The calculation of three pairs of M and ϕ values plus a fourth limiting M value will satisfactorily determine the curve for a WF section at various states of yielding as follows:

M_1, ϕ_1 at initial plastic yielding of outer fibers of beam

M_2, ϕ_2 after yielding has progressed through the flange to the juncture of web and fillets (to y_2 in Fig. 1 (b))

M_3, ϕ_3 after yielding has progressed into the web any appreciable amount (to y_3 in Fig. 1 (b))

M_4 . . the limiting moment assuming the entire section to be plastic

It will be assumed that initial yielding takes place when the most stressed fibers in bending reach a stress equal to the upper yield point of the flange material σ_{UYF} as determined by a tension or compression test.

As soon as yielding has commenced it is questionable whether the upper yield point should be assumed as maintained on the elastic side of the theoretical elastic-plastic boundary. The material used in this investigation had an upper yield point not much larger than the lower and no conclusions could be drawn as to the foregoing matter. The two different procedures would give nearly identical curves and in the absence of conclusive evidence it will be assumed that the upper yield point is maintained at the elastic plastic boundary, and that the lower yield point obtains throughout the plastic region, as shown in Fig. 1 (b).

In the Appendix the formulas are developed for calculating M and ϕ at the four stages of plastic yielding and an illustrative example is presented of the M-ϕ curve of the 8WF67 section having handbook dimensions and a minimum specification yield point of 33 ksi.

Figure 2 shows this M-ϕ curve along with the M-ϕ curve for a rectangular section having the same depth and the same section modulus as the 8WF67, 9 in. deep by 4.474 in. wide.

Shape of Cross Section

The ratio of the limiting moment with

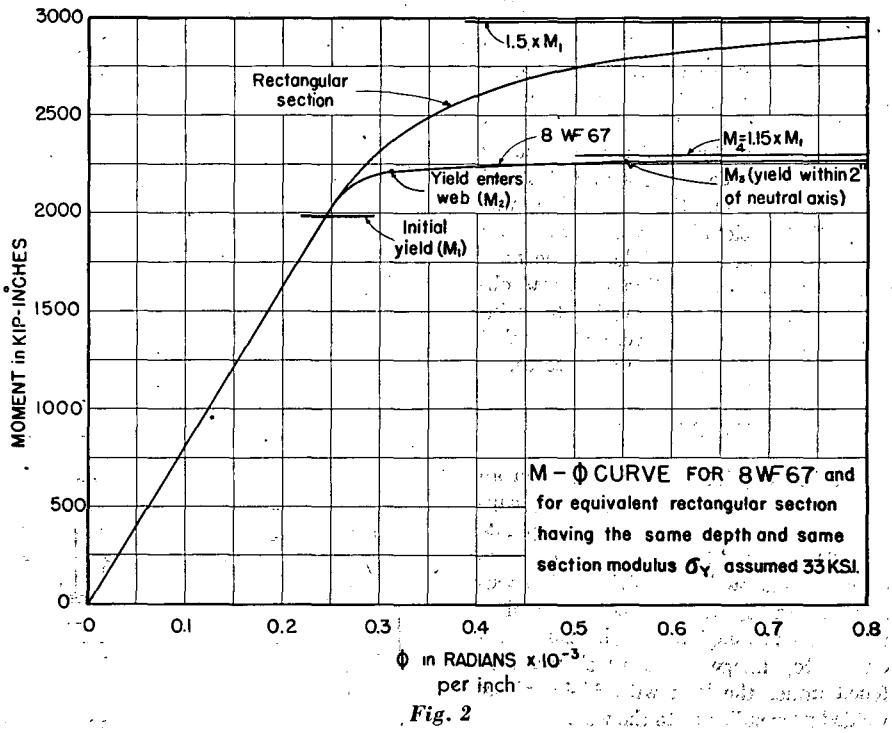

Fig. 2

* Reference should also be made [2,3] to other basic assumptions made in the beam theory.

the whole section assumed plastic (M_4), divided by the moment at initial yield (M_1), is sometimes called the "shape factor" of the section. This is an index of the plastic reserve strength of a particular cross section, being 1.50 for the rectangular shape and 1.15 for the 8WF67 section, both of which have the same moment at initial yield.

As typified in Fig. 2, the I-beam or WF shape has an M-ϕ curve with a sharp knee at moments 5 to 15% larger than the maximum elastic moment. Thereafter, ϕ increases very rapidly at nearly constant moment and the beam becomes, in effect, a "plastic hinge." The computation of ultimate or collapse loads of continuous frames is simplified by assuming the development of plastic hinges at successive locations of maximum moment in the structure.

Local Buckling

If the outstanding parts of the flange buckle before reaching the yield point, or, if plastic buckling occurs shortly after the section yields, the full contribution of the plastic hinge to the ultimate strength of the continuous frame will not be realized. However, all currently rolled structural shapes as listed in the *A.I.S.C. Handbook* have a flange thickness sufficient to insure against elastic buckling, and will develop the full yield strength of structural steel. However, if higher strength or nonferrous alloys are used, or if thin sections are built up by welding, the problem of local buckling should be given consideration as has been done in a recent investigation.[5]

Residual Stresses

Residual stresses are generally thought to have little or no effect on the static strength of structural steel members. In many instances this has been demonstrated; however, at least one investigator[6] has reported a lowering of buckling strength due to internal stresses caused by welding. After completing pilot tests of this investigation, the suggestion was made that residual stresses caused by rolling might be responsible for the nonuniform strain distribution that was observed. Therefore, the regular tests included specimens that were stress-relief annealed after welding of test fixtures.

PILOT TESTS

The initial pilot test was made on an 8WF40 beam of 12-ft. span, simply supported and loaded at the third points (Fig. 3). Around the center section of the beam were located 18 electric strain gages as shown in Fig. 4. The load was applied to the beam through bearing blocks resting on the top flange and the web was stiffened under the load with $^3/_8$-in. plates welded perpendicular to the web.

Upon testing this specimen it was observed that, when the elastic limit of the beam was passed, the strain across the center section no longer followed a straight line variation. The strain in the compression flange remained relatively constant from the 46 to 52 kip load while the strain in the web and tension flange progressed and the neutral axis moved toward the tension flange. This phenomenon can be observed in Fig. 4. This figure also shows that the neutral axis

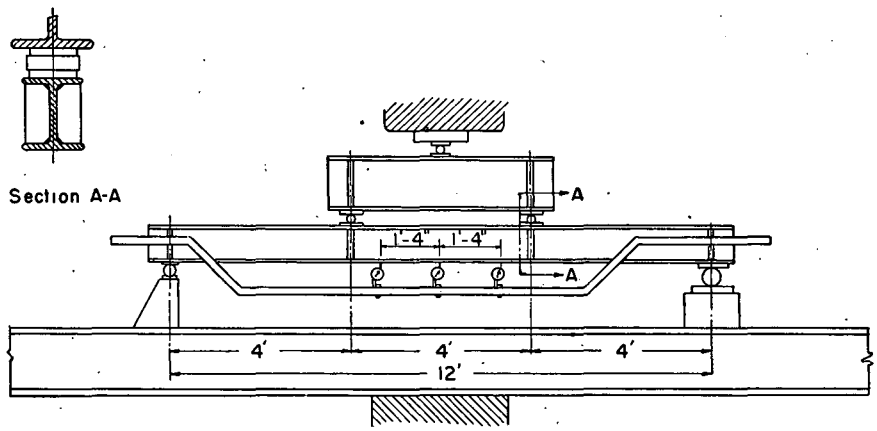

Fig. 3 Set up of pilot tests

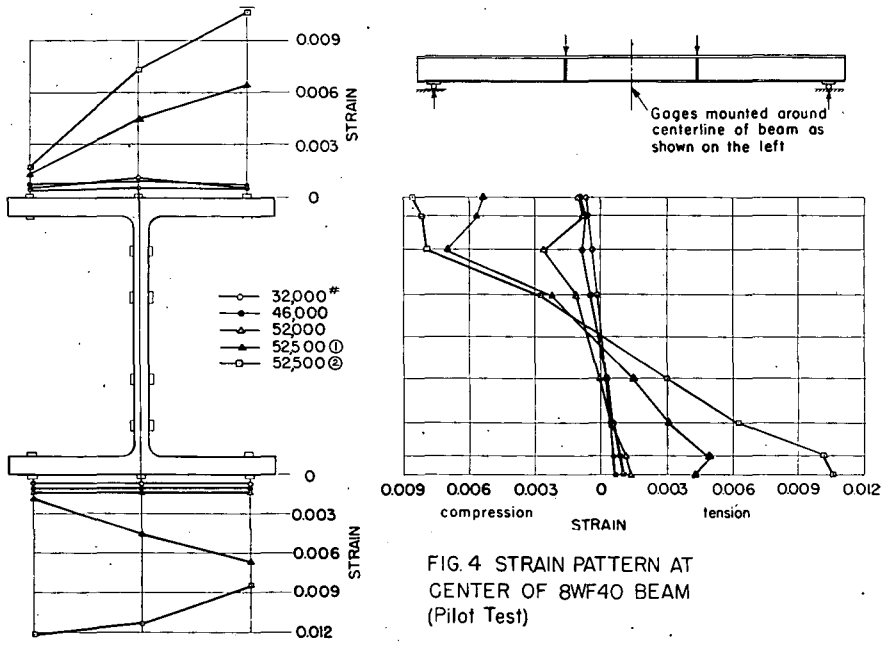

FIG. 4 STRAIN PATTERN AT CENTER OF 8WF40 BEAM (Pilot Test)

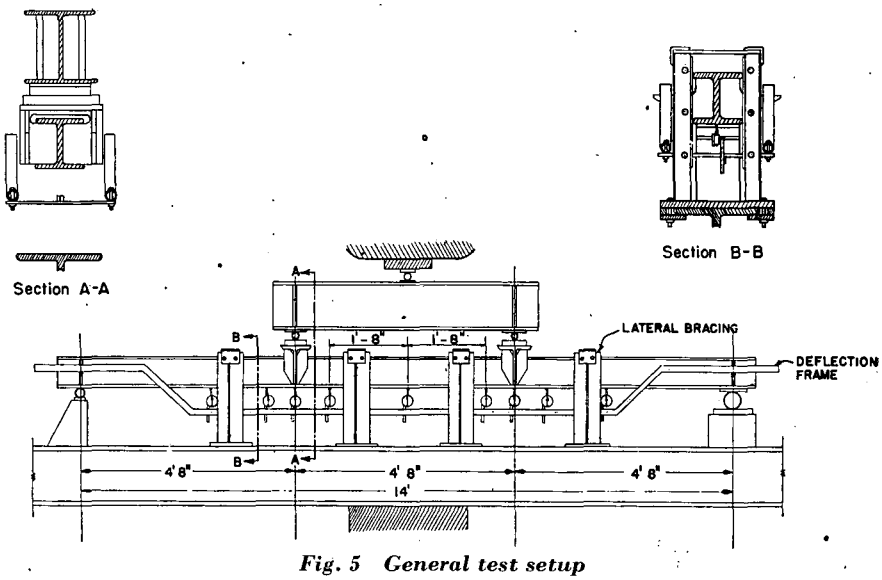

Fig. 5 General test setup

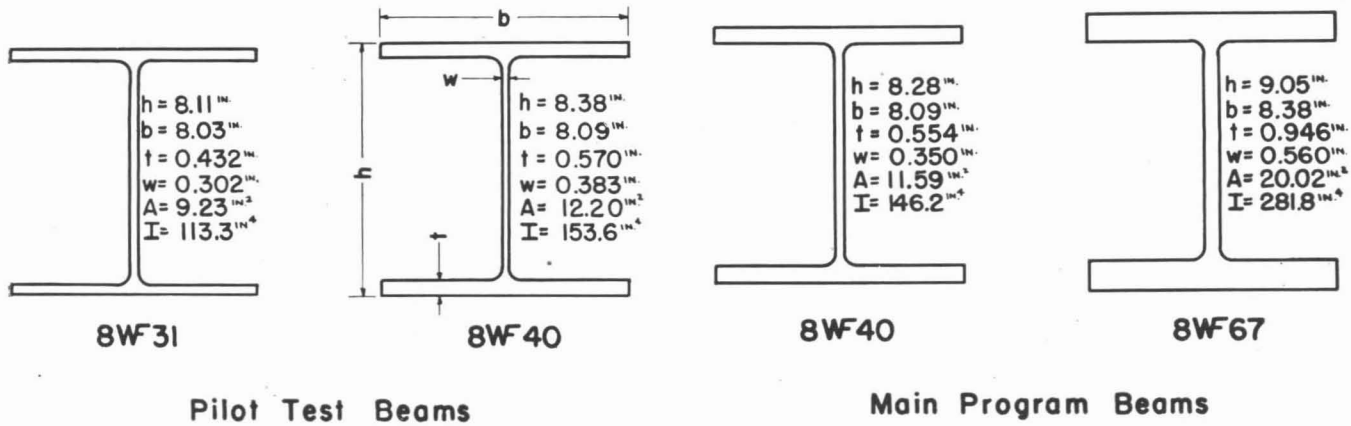

Fig. 6 Dimensions and properties of cross section of beams

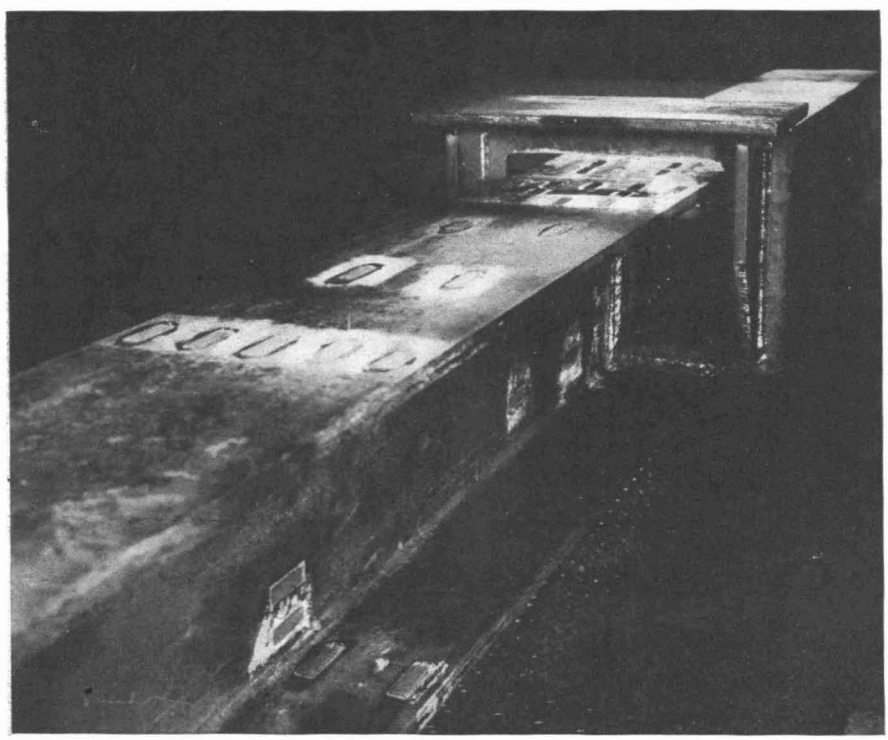

Fig. 7 Load carriers and S-R4 gages prior to connecting

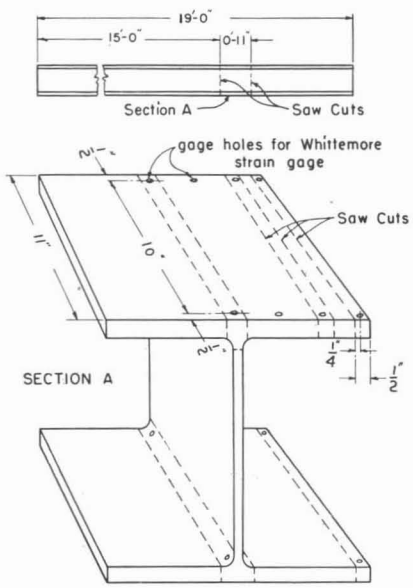

Fig. 8 Representation of how residual strain measurements were obtained

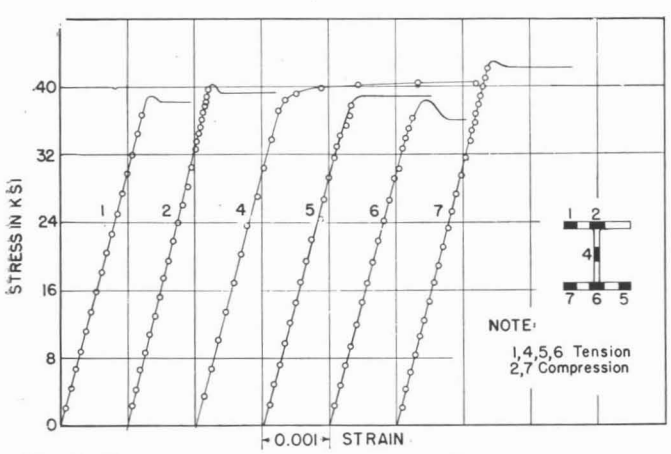

Fig. 9 Stress-strain curves for physical property coupons of 8WF31 pilot test beam

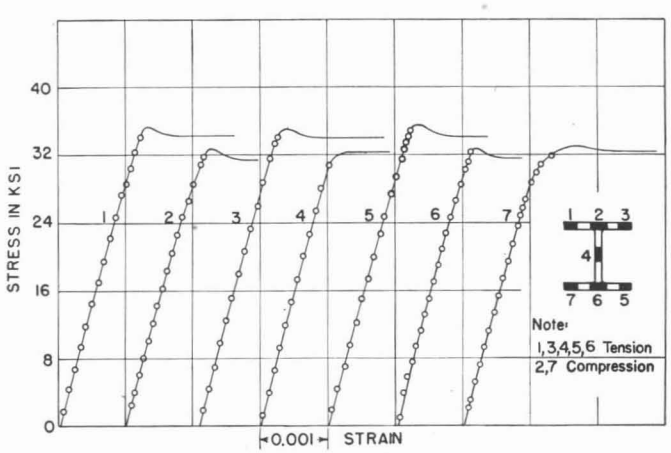

Fig. 10 Stress-strain curves for physical property coupons of 8WF40 pilot test beam

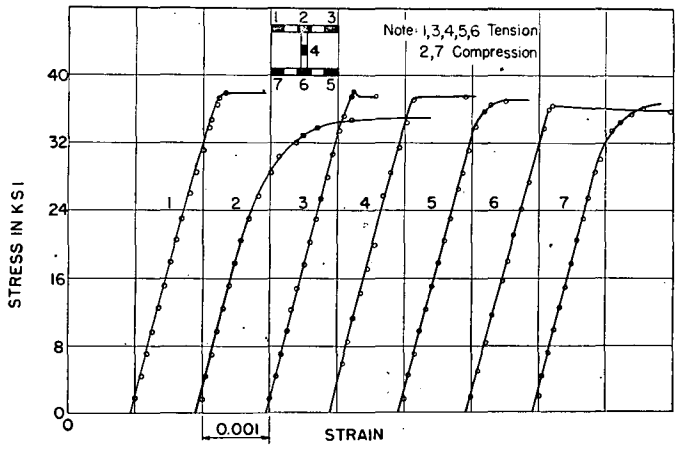

Fig. 11 Stress-strain curves for physical property coupons of 8WF40 as-delivered beam

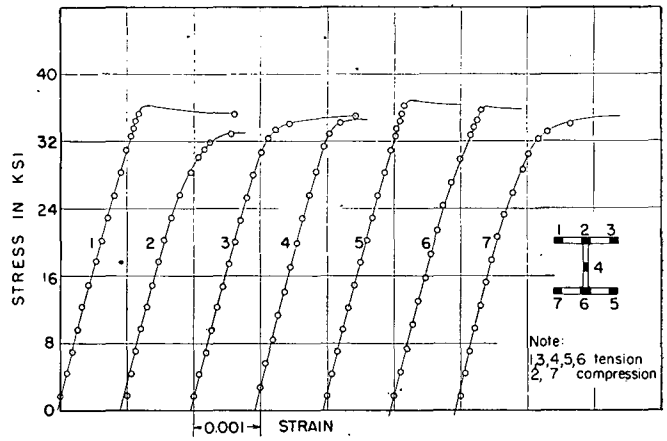

Fig. 12 Stress-strain curves for physical property coupons of 8WF40 stress-relieved beam

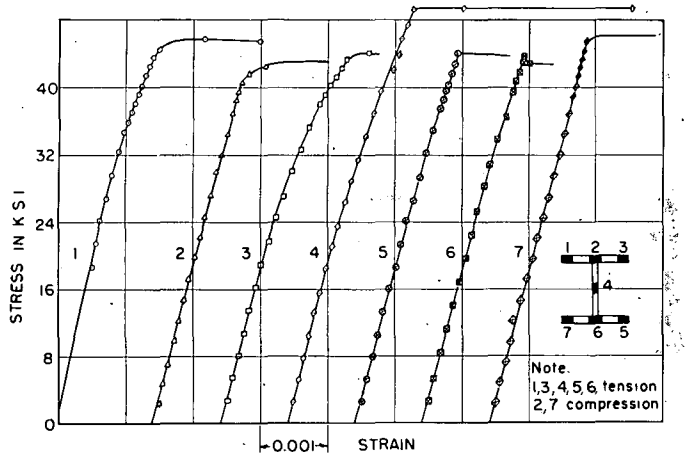

Fig. 13 Stress-strain curves for physical property coupons of 8WF67 as-delivered beam

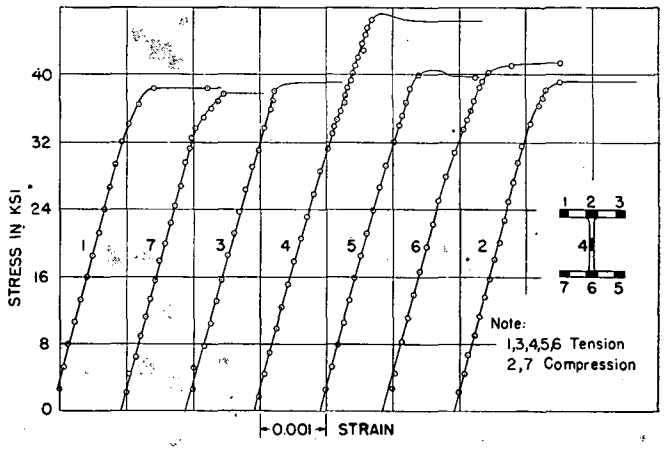

Fig. 14 Stress-strain curves for physical property coupons of 8WF67 stress-relieved beam

moved back toward the centroidal axis of the beam at higher per cent strains. The pilot test developed less plastic strength than that calculated. This fact, together with the nonlinearity observed in the strain distribution, led to the decision by the committee to carry out a more detailed study of additional beam tests.

PROGRAM OF TESTS

The four "regular tests" had as objectives: (1) to thoroughly study the strain pattern throughout the beam for increasing degrees of plastic development, and (2) to compare the M-ϕ curves obtained from tests with theoretical curves predicted from tension and compression tests.

Two variables were incorporated into the four tests, namely: (1) the effect of residual stress, and (2) the effect of the geometry of the section on its behavior. To obtain these variables two 8WF40 and two 8WF67 beams were tested and in each weight one beam was tested in the as-delivered condition and the other was stress-relief annealed prior to testing.

The method of load application was made to simulate a beam-to-girder connection by bringing the load directly into the web as is depicted in Figs. 5 and 7. This method of applying the load to the beam differed from the flange bearing block method used in the pilot tests, as previously described and as shown in Fig. 3.

PREPARATION OF SPECIMENS

Initial Preparations

Except for the stress-relief annealing process each beam was prepared for testing in the same manner. Upon receiving the

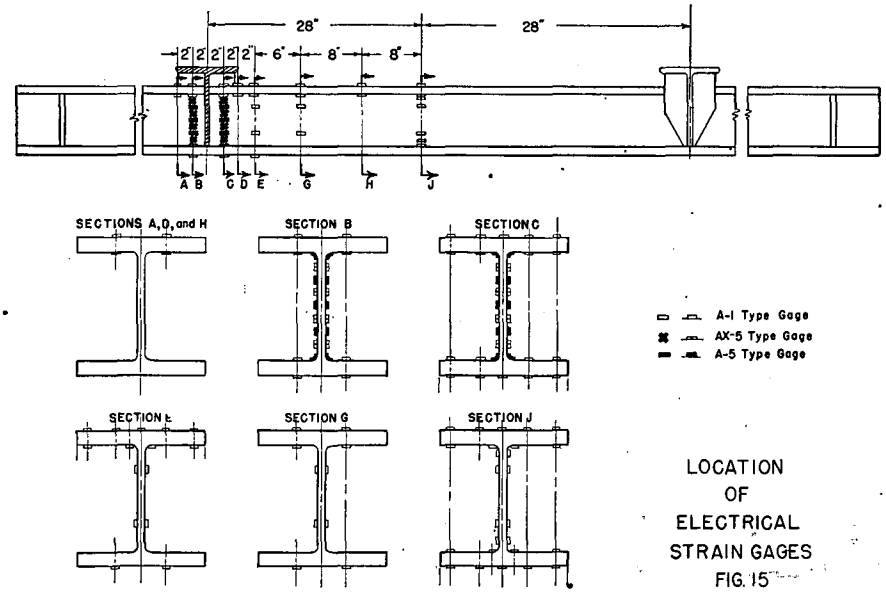

LOCATION OF ELECTRICAL STRAIN GAGES
FIG. 15

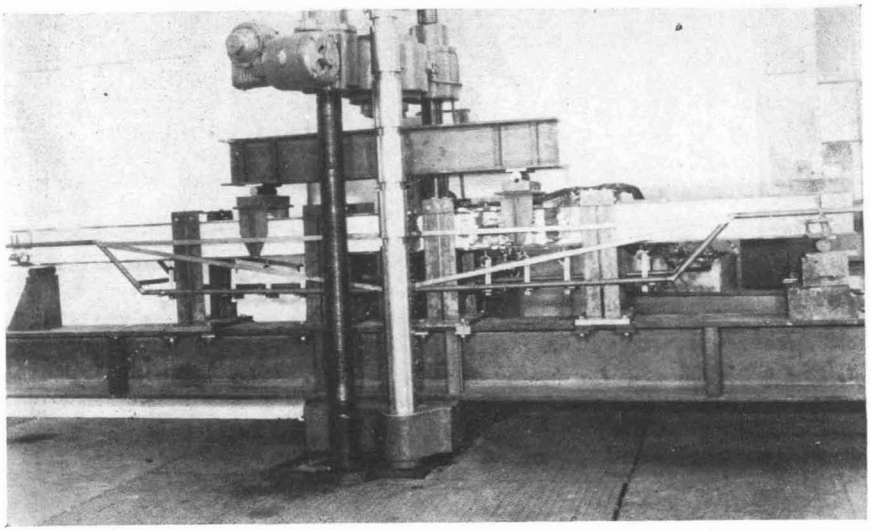

Fig. 16 General view of typical test setup prior to testing

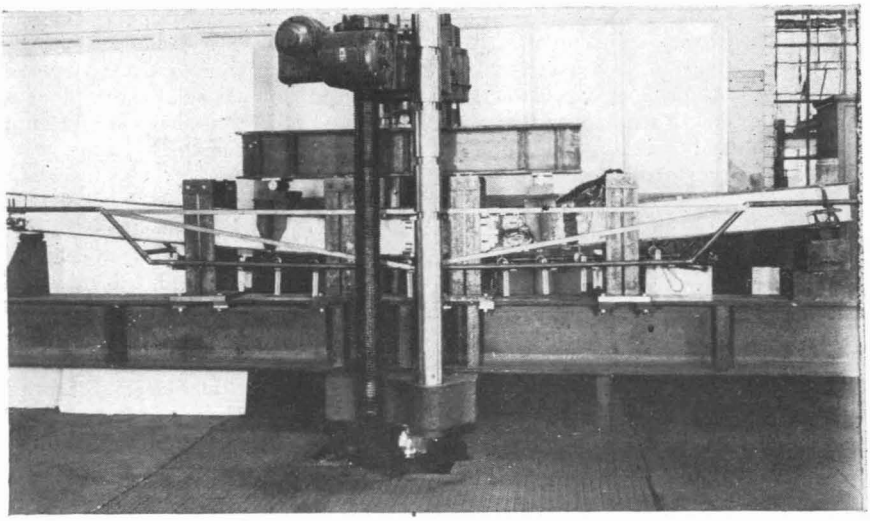

Fig. 17 Same as Fig. 16 after testing

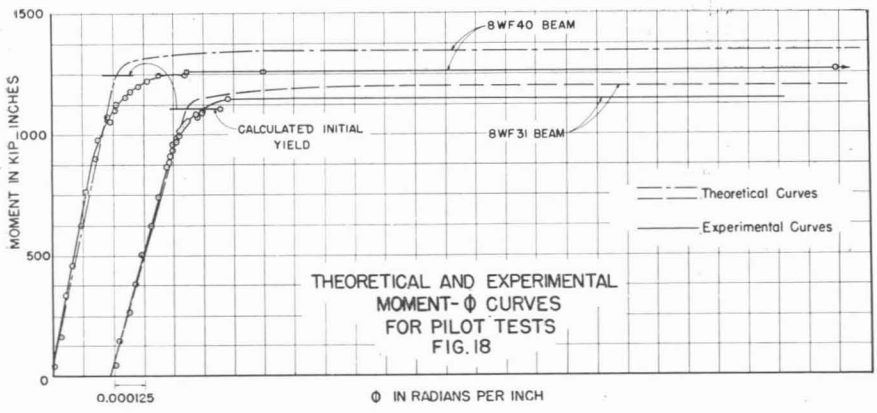

Table 1—Average Results of Tension and Compression Tests, Ksi.

	Pilot tests		*Regular series*			
	8WF31, as-delivered	*8WF40, as-delivered*	*8WF40, as-delivered*	*8WF40, annealed*	*8WF67, as-delivered*	*8WF67, annealed*
σ_{UYF} (5 or 6 tests, av.)	40.04	34.08	36.85	35.53	44.38	39.40
σ_{UYW} (one test)	40.50	32.40	37.40	34.65	49.40	47.20
σ_{LYF} (5 or 6 tests, av.)	39.04	32.98	36.50	34.96	43.93	39.20
σ_{LYW} (one test)	40.50	32.20	37.20	34.65	49.20	46.30

beams in the laboratory they were weighed and measured. The cross-sectional area was determined from the weight and length and used to check the direct measurements by micrometer calipers. The dimensions and calculated properties of the sections are shown in Fig. 6.

The load-carriers and stiffeners over the supports (Figs. 5 and 7) were welded in position and then the beams to be stress-relief annealed were delivered to the shop for this process. The next step was to determine the residual strains in the beams.

Residual Strain Measurements

The specimens had been ordered in 19-ft. lengths, 4 ft. longer than required for the beam tests. This four extra feet had the twofold purpose of being used for residual strain tests and also as coupons for physical property tests. The following procedure was used in determining the residual strains in the beams.

On the 19-ft. length the 15 ft. required for the beam test was laid out from one end. Adjacent to this (Fig. 8) the desired number of 10-in. gage lengths were laid out around the beam section and the Whittemore strain gage holes were drilled, prepared and a complete set of readings taken around the section. The portion *A* in Fig. 8 was then sawed out of the 19-ft. length, and finally all the gage lengths were isolated by sawing $^1/_4$ in. on either side of each pair of holes. Readings were then taken on these isolated lengths and relaxation of strain computed. Although the accuracy of the method was not perfect, the results obtained indicate the magnitude of the residual strains in the beams.

In the first beam tested for residual strains (8WF40 as-delivered), measurements were taken only for one half of the section with a few check points on the other half. However, it was decided after this test that more points for measurements were required, and therefore in the specimens that followed either 44 or 46 points of measurement were used.

Physical Property Tests

The remaining 3 ft. of the original 19-ft. length was used to make physical property coupons which would be, of course, representative of each beam. Seven coupons were taken from each section located as shown in Figs. 9 to 14, which present all stress-strain curves. The upper and lower yield points of the web and flange were used in equations 2 to 8 (Appendix) to determine the theoretical curves. Table 1 gives a summary of the average physical properties of all the coupon specimens. As shown by Figs. 9 to 14, tension and compression tests were usually in close agreement and the over-all average of the six flange coupons was used to determine σ_{UYF} and σ_{LYF} as used in calculating the theoretical M-ϕ curves.

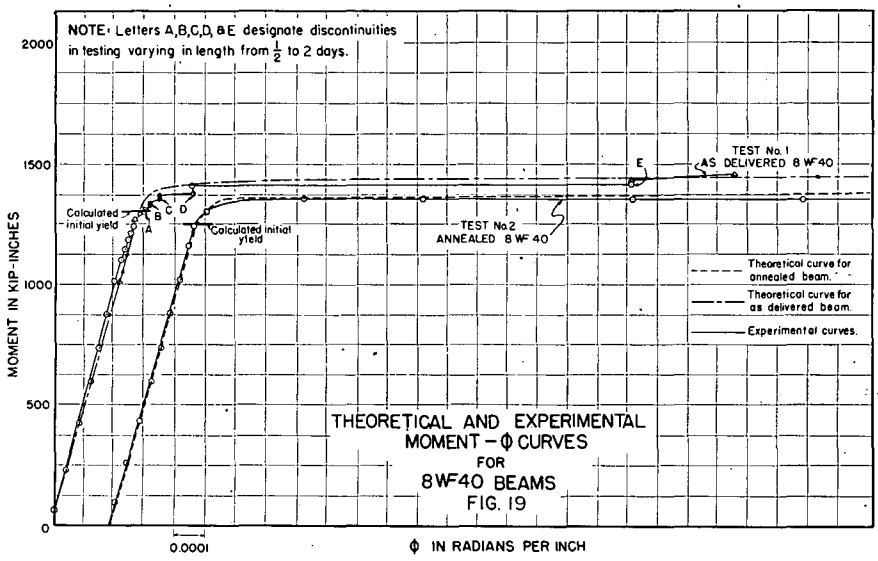

An O. S. Peters strain gage of 2-in. gage length was used for tension tests and two Huggenberger tensometers were used for compression specimens. A modulus of elasticity of 30,000 ksi. was used in all calculations and was representative of the test results.

Electrical Strain Gages

The next step in the preparation of the beams prior to testing was to lay out the electrical, SR-4, strain gage locations.

In order to thoroughly study the strain pattern developed around the loading point and the region of pure bending, 141 electrical strain gages were mounted on each beam specimen in the pattern shown in Fig. 15. Gages were mounted only on one half of the beam, since the results obtained should be similar in both sides. AX-5 gages were used along with uniaxial gages in the vicinity of the load carrier to allow a complete study of strain that might develop from bending, shear or be the result of the concentration of load in the area. Uniaxial gages were mounted along the beam at various points to permit measurement of the longitudinal strain across different sections in the pure bending region, and to enable a study to be made of any change in strain pattern along the beam which might be attributed to the position of the section in this pure bending region.

After completing the mounting of SR-4 gages and their wiring, the specimens were ready for testing and were set up in the 300,000-lb. Baldwin-Southwark hydraulic testing machine. A Baldwin-Southwark Type K strain indicator was used to measure strains in conjunction with switch boxes made at the Fritz Laboratory. Figures 16 and 17 are photographs of the complete setup before and after one of the tests.

Deflection Gages

As illustrated in Figs. 5 and 16 deflections were measured at nine points along the beam by means of dial gages. Three of these dial gages were mounted in the pure bending region of the beam to enable calculations to be made of the rotation or angle change due to the applied moment in the section and to allow plotting of observed M-ϕ curves for all the beams.

Lateral Bracing

In the pilot tests considerable lateral deflection, as well as twisting, developed as the beam progressed into the plastic range. Lateral bracing was supplied to the regular test specimens by forming an adjustable, vertical passageway for the beams as is illustrated in Fig. 5. The distances between the guide plates at the bottom and top were carefully measured to be sure that the plates were parallel as well as vertical, to insure against pinching of the beam as it deflected. These plates were also greased so that friction between the vertical slides and the beam would be a minimum.

Whitewash

The final preparation prior to test was to paint slaked lime whitewash on the beams. This whitewash served as an aid in studying the progression of yielding throughout the specimens.

TEST PROCEDURE

The testing procedure for all the specimens was as similar as possible. However, regular test 1, 8WF40, as-delivered, was run at perhaps a slower rate than was justified. This factor, along with unavoidable interruptions in the test, and the length of time involved in recording the 141 strain gage and nine deflection readings, caused the test to extend over a period of approximately two weeks. Beyond the yield point there were observed numerous discontinuous increases in strength of the member which are attributed to strain aging.

The remaining three beam tests were planned so that it would not be necessary to interrupt the early stages of plastic development, thereby reducing strain aging as much as possible. To accomplish this the tests were carried to within a safe margin of the calculated elastic limit on the first day of testing and the entire second day was used to carry the test well into the plastic region. In comparison to the first test the other three extended over the following lengths of time: 8WF40 annealed, 2 days; 8WF67 as-delivered, 3 days; 8WF67 annealed, 4 days.

In all the tests, readings were recorded when the deflection of the beams stopped or the rate of deflection became a negligible amount for a particular load.* Strain and deflection were also recorded at intervals before these values were reached to indicate the progression of yielding under a constant load. To obtain readings which would give the strain and deflection pattern for the entire beam at a particular instant even though the beam was in the process of yielding, the load was dropped slightly to stop yielding. Then a complete set of readings was recorded. The amount that the load had to be dropped to accomplish this was small and the reduction in

* An equilibrium condition was assumed when the deflection in the center did not increase more than 0.02 in. in 30 min.

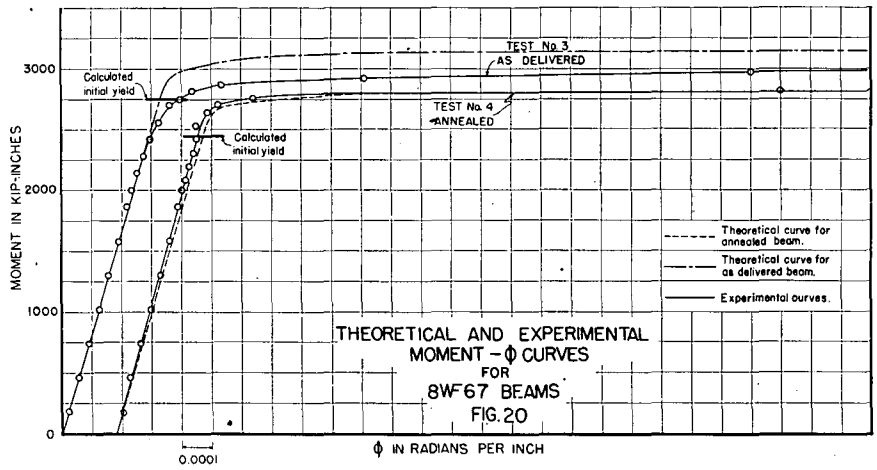

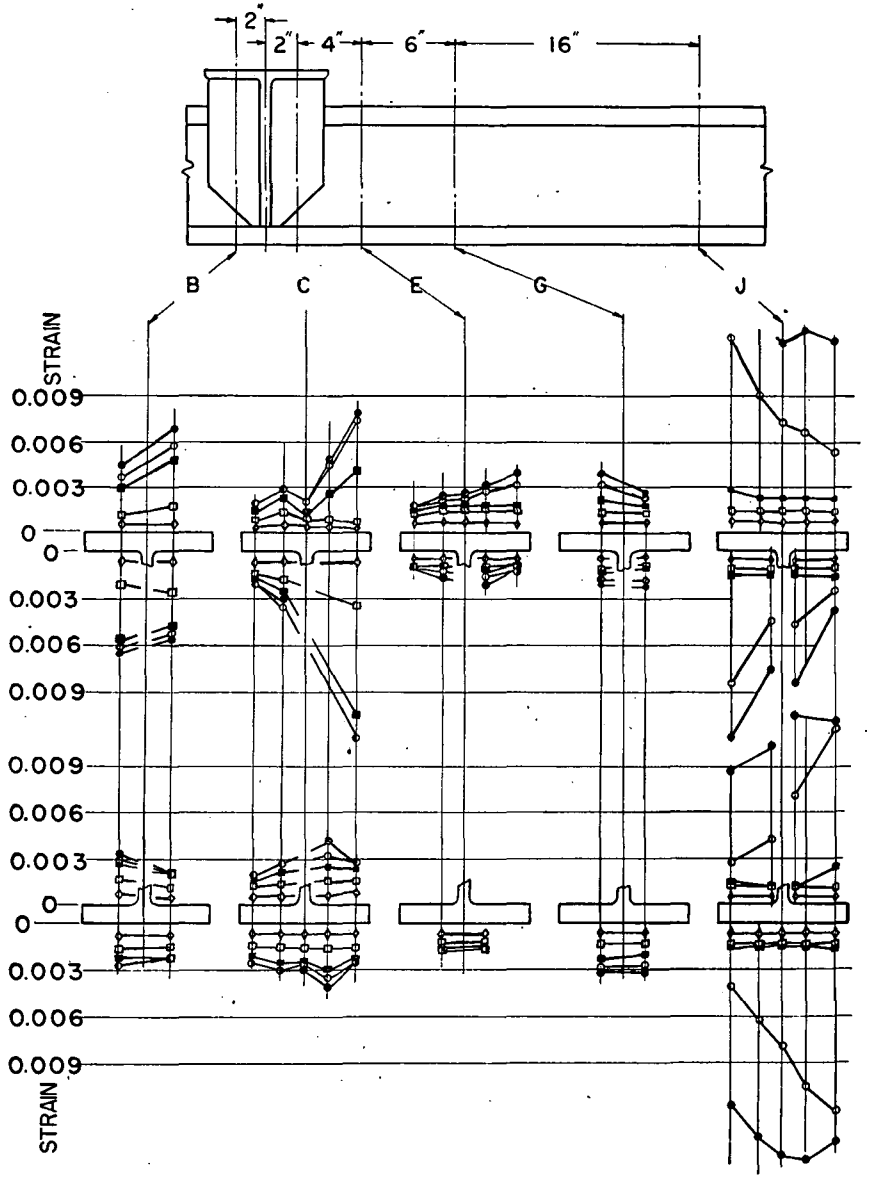

FIG. 21 STRAIN ACROSS FLANGES OF 8 WF67 AS DELIVERED BEAM

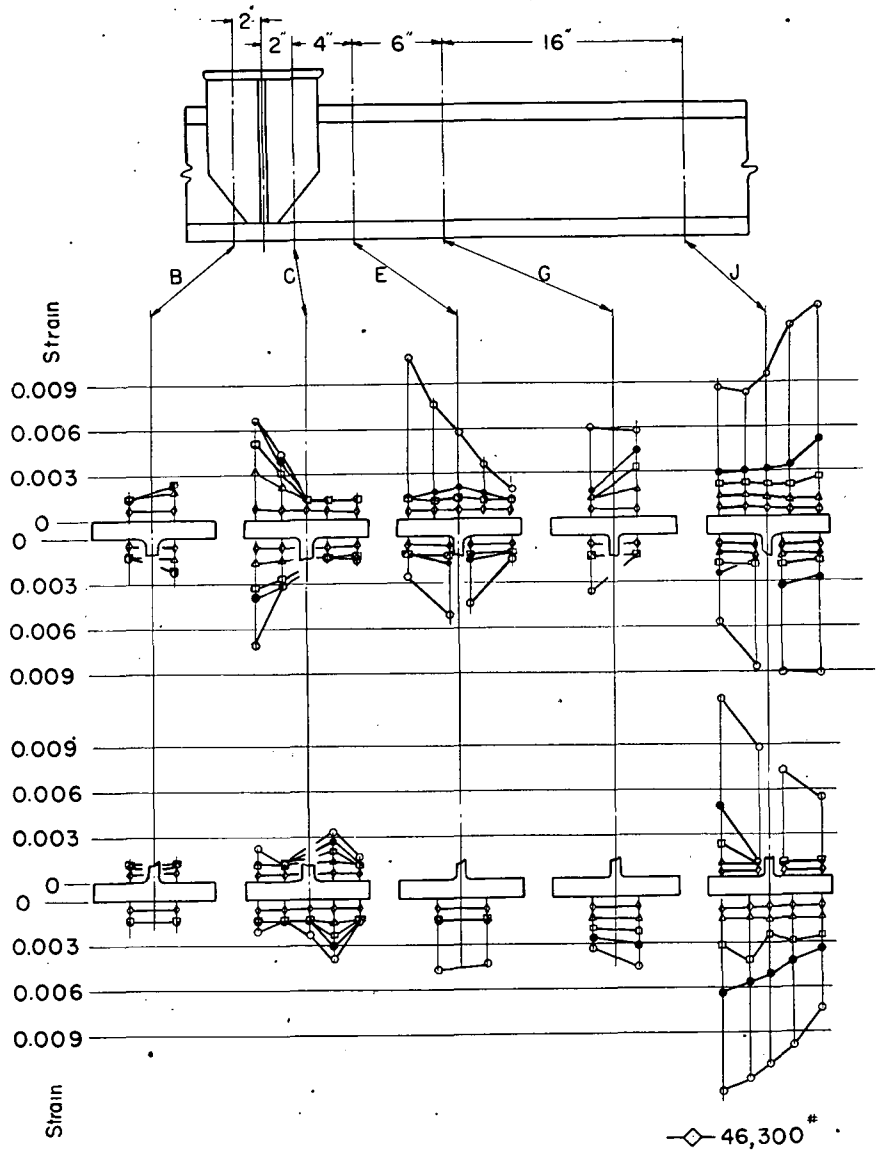

FIG. 22 STRAIN ACROSS FLANGES OF 8WF67 ANNEALED BEAM

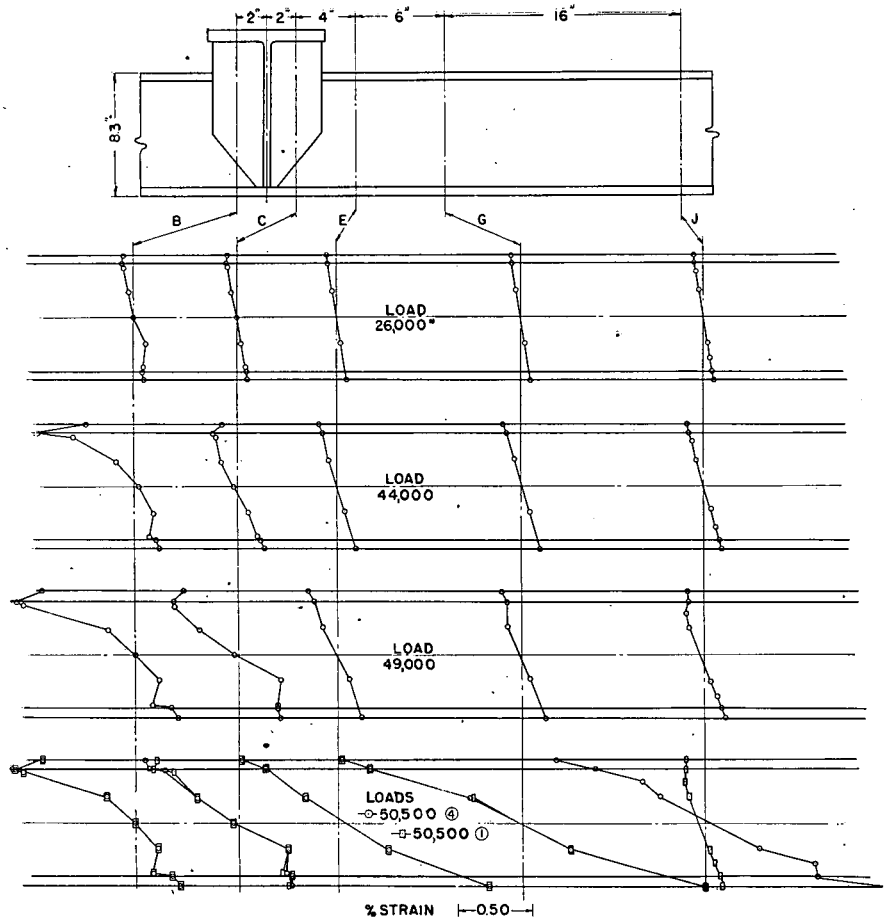

Fig. 23 Strain on various cross sections along as-delivered 8WF40 beam

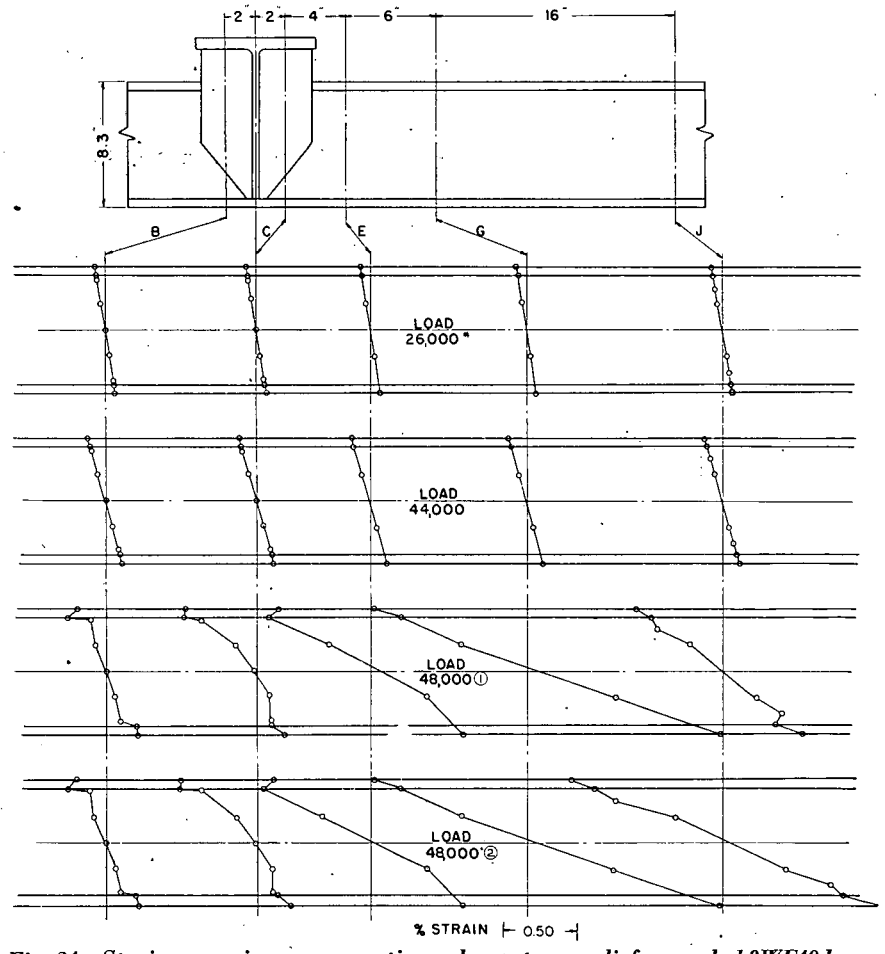

Fig. 24 Strain on various cross sections along stress-relief annealed 8WF40 beam

strain, at the elastic rate, was a negligible value which could not be seen on the plotted curves.

When it became necessary to interrupt the testing for a considerable length of time, overnight for example, the hydraulic testing machine was shut down with the load left on the specimen. This was done to keep as much load on the specimen as possible to prevent any recovery that might tend to occur. However, over a period of 12 hr. the load would drop to about two-thirds of the original value, due to gradual seepage of oil from the hydraulic testing machine loading cylinder.

All tests were carried far enough so that the beams should have developed nearly all of their ultimate plastic hinge value prior to general strain-hardening.

TEST RESULTS

Results of the moment-curvature relation, or M-ϕ diagrams are presented in Figs. 18–20 for the pilot tests, 8WF40 tests and 8WF67 tests, respectively. Actual test curves are compared with curves determined theoretically by the procedure outlined in the introduction and appendix. These curves illustrate the bending behavior of the specimens and determine their plastic hinge value.

Longitudinal strain gage data at various loads are presented graphically for typical test results as follows:

Fig.

21 Strain across flanges of 8WF67 as-delivered beam

22 Strain across flanges of 8WF67 annealed beam

23 Strain on various cross sections along as-delivered 8WF40 beam

24 Strain on various cross sections along annealed 8WF40 beam

25 Strain distribution along tension flange of 8WF67 beam

26 Strain distribution along compression flange of 8WF67 beam

In each of the three foregoing categories the data from one beam size is omitted, but is available in the original report at Fritz Laboratory. Figures 21 and 22 show the strain distribution on the flanges of the 8WF67 beams at various loads and degrees of plastic development. The 46,300-lb. load is approximately equivalent to a maximum fiber stress in the beams of 20,000 psi., while the subsequent loads for plotting curves were chosen at or above the apparent elastic limit of the material. There appears to be little if any difference in the curves for the stress-relief annealed and the as-delivered beams which might be attributed to residual stress, except around the load carrier, where residual stresses of apparently greater magnitude than elsewhere existed because of welding. (Note the surface yield lines shown in Fig. 27.)

The strain distribution at points along the 8WF40 beams for different loads and

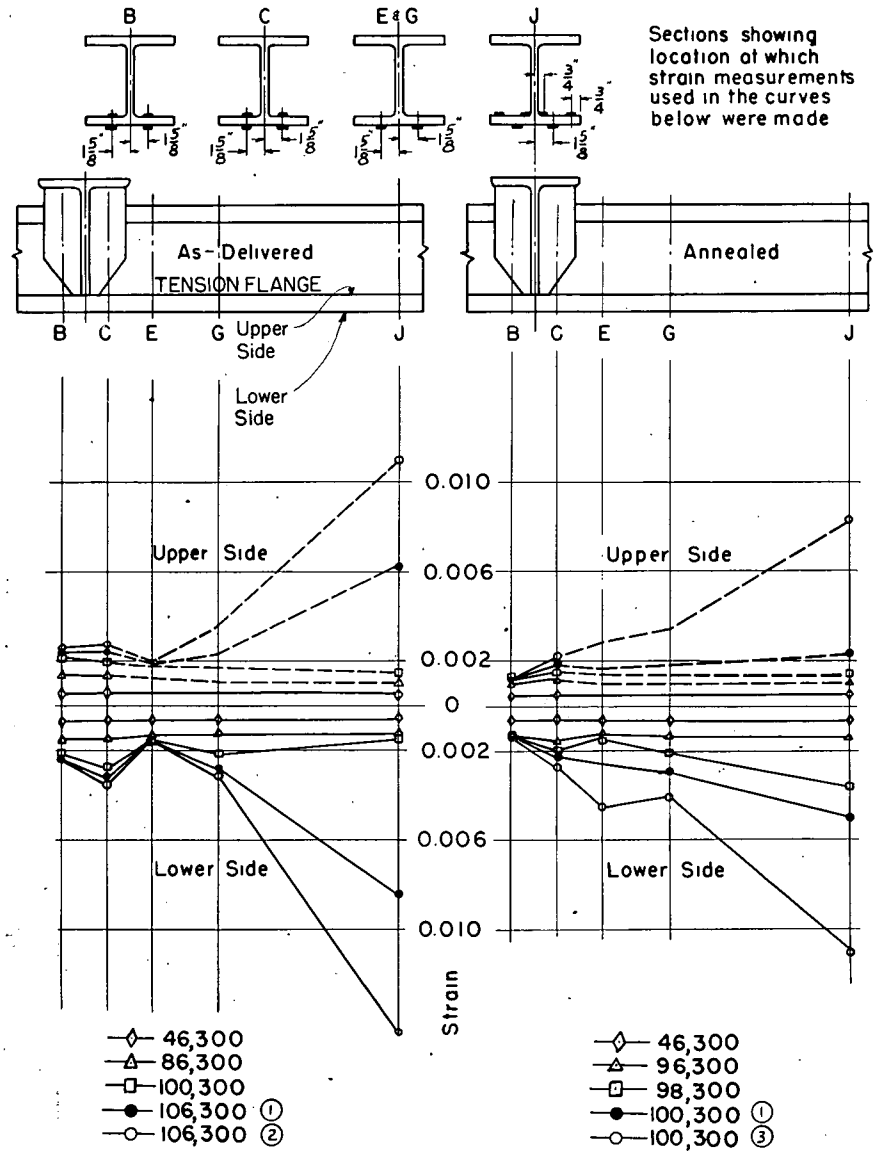

FIG. 25 STRAIN DISTRIBUTION ALONG TENSION FLANGE OF 8WF67 BEAMS

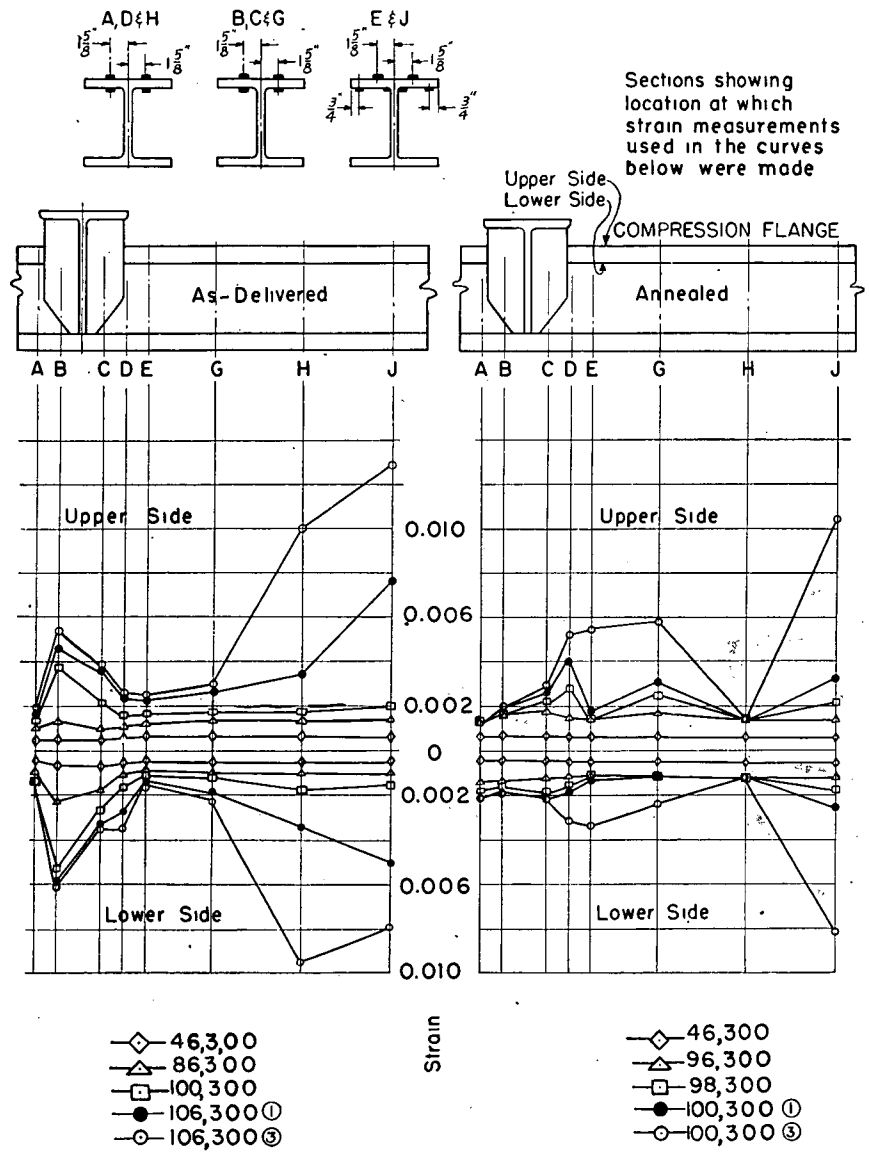

FIG. 26 STRAIN DISTRIBUTION ALONG COMPRESSION FLANGE OF 8 WF67 FLANGE

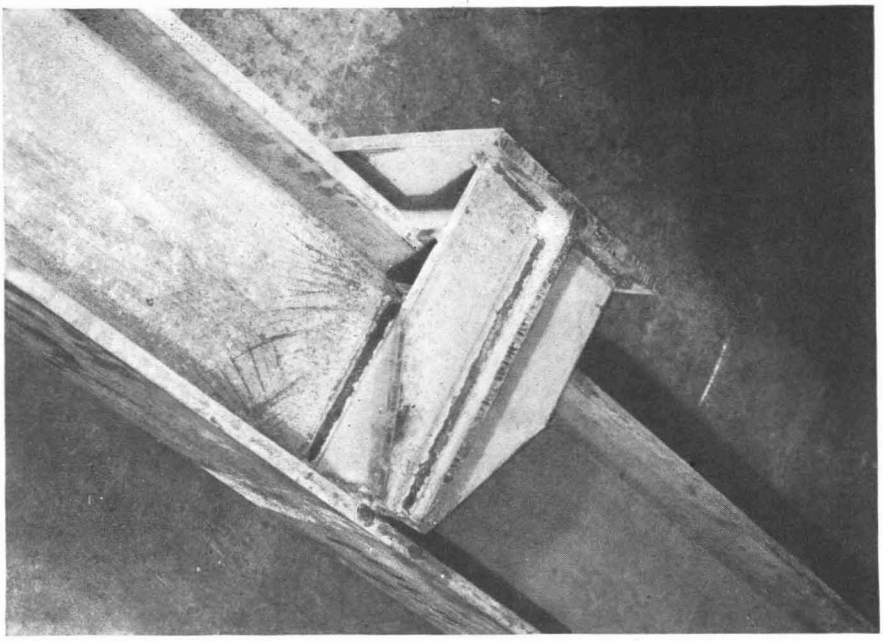

Fig. 27 Surface yield lines produced by welding load carrying stiffeners

degrees of plastic development are shown in Figs. 23 and 24. The values plotted in these figures are averages of all the gages occupying the same position vertically on the section. These curves show no appreciable difference which might be attributed to the variables studied, except as mentioned before there is initial yielding around the load points at a much lower load in the as-delivered beams than the annealed beams. It can be observed in these figures also that the strain distribution even in the vicinity of the load point is linear through the elastic ranges but that once the yielding starts there is considerable deviation from linearity. These figures also illustrate the change of strain pattern or flow of the material under a particular load. For example, in Fig. 23 there are shown two sets of curves for the load of 50,500 lb. obtained before and after a lapse of time. As can be seen from these curves, yielding at Section J did not occur until yielding at sections B, C, E and G had very nearly stopped. Progression of yielding under one particular load is also illustrated for the annealed 8WF40 in Fig. 24. (See also Figs. 32 and 33.)

A study of the degree of yielding along the beams is depicted by Figs. 25 and 26. These figures show the average strain developed in the flanges of the 8WF67 beams under increasing loads. Here also is shown that the point of maximum plastic strain does not occur at the loading point but rather that yielding seems to be retarded in this section and the region of maximum yielding occurs from about 6 in. inside the loading point to the center of the beams. However, there was appreciably more yielding at the load point in the as-delivered beams than in the annealed beams.

The residual strains caused by rolling and handling in the as-delivered and stress-relief annealed beams as determined by the method previously described are presented in Figs. 28 and 29. The sections at the top of these figures are oriented so that referring to the test setup the person is looking at the left end of the beam toward the far end. Subsequently the views labeled *B* are taken looking into the near side of the beams as shown in various figures illustrating the test setup. All figures portraying strain are oriented in this way so that the strain measured under load may be studied and compared directly with the residual strain patterns.

Progression of Yielding Indicated from Whitewash

Since in a general manner the progression of yielding in all the specimens was similar, a complete discussion of the progression of yielding observed in one of the beams will be representative of all.

The following is the complete history of yielding in the 8WF67 stress-relief annealed beam, Test 4, as observed by cracking of the whitewash on the beam.

At a load of 90,300 lb., the first sign of yielding appeared on the compression flange at the loading point of the beam. When the load was increased to 94,300 lb., indications of yielding occurred on both the top and bottom of the compression flange in the vicinity of the load point, and initial yielding appeared in the compression flange inside of this region as is shown by Fig. 30 (*a*). These yield lines appeared simultaneously on the bottom and top of the compression flange. Figure 30 (*b*) shows the yield lines in the compression flange 1 hr. after applying 96,300 lb. to the beam, and Fig. 30 (*c*) gives the same view several hours later at the same load. Figure 31 (*a*) shows the condition in the region of the load carrier at the same time. Both Figs. 30 (*c*) and 31 (*a*) were taken after the beam had stopped yielding under the applied load. One hour after the application of 98,300 lb., the beam appeared as is shown by Figs. 31 (*b*), 32 (*a*) and 33 (*a*).

After a lapse of 5 hr., the final yielded condition under the load of 98,300 lb. is shown by Figs. 32 (*b*) and 33 (*b*). Figures 32 (*c*) and 33(*c*) show the beam $^1/_2$ hr. after application of the ultimate load of 100,300 lb. Finally Figs. 34, 35 and 36 show the beam at the completion of the test.

The similarity of the progression of yielding in the different tests is shown by Figs. 37 to 40. Figure 37 shows initial yielding and Fig. 38 the final appearance in Test 1 of the 8WF40 as-delivered beam. Figure 39 shows the final appearance of the 8WF40 stress-relief annealed beam, and although no pictures are available it can be stated that yielding first appeared in the form of flaking whitewash at the same location as it occurred in the as-delivered beam of this weight, and as shown by Fig. 37. Initial yielding in Test 3 of the 8WF67 as-delivered beam, as observed from the whitewash, occurred at the junction of the web, bottom flange and load carrier. Final appearance of this beam is shown in Fig. 40.

In general with regard to the yielding of these beams it can be said that yielding first occurred in the vicinity of the load point, although it did not spread into the pure bending region from this point. Secondly, yielding would appear at some point on the top flange inside the loading points and spread throughout the top flange and into the web to some degree before indication of yield lines would appear on the bottom flange. This progression would continue, then, until it reached the final condition as shown in previously mentioned figures.

Not all of the studies to be made of these tests results have been completed for this first progress report. A study of the local stresses near the load bearing stiffeners and the complete deflection curve results are omitted.

SUMMARY AND CONCLUSIONS

The agreement between the experimental and calculated M-ϕ curves is as good as could possibly be expected in the case of tests 2 and 4 of the annealed 8WF40 and 67 beams, respectively, as shown in Figs. 19 and 20. The test M-ϕ curves for the two pilot tests are somewhat lower than the curves calculated from the stress-strain diagrams; however, the pilot tests differed from tests 2 and 4 in the following respects: (1) Pilot test beams were not annealed, (2) were not laterally supported and (3) were loaded with bearing blocks through the top flange whereas

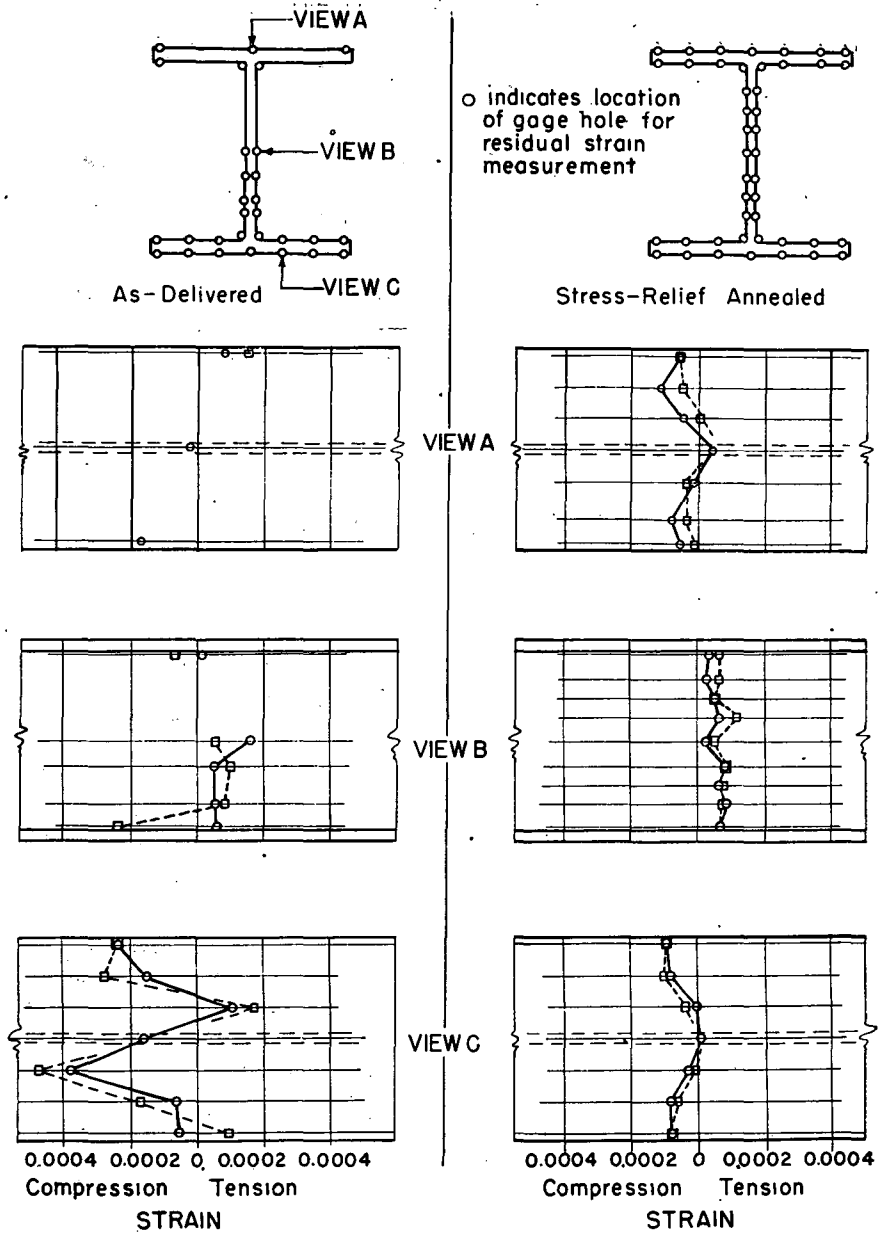

FIG.28 RESIDUAL STRAIN IN 8 WF40 BEAM

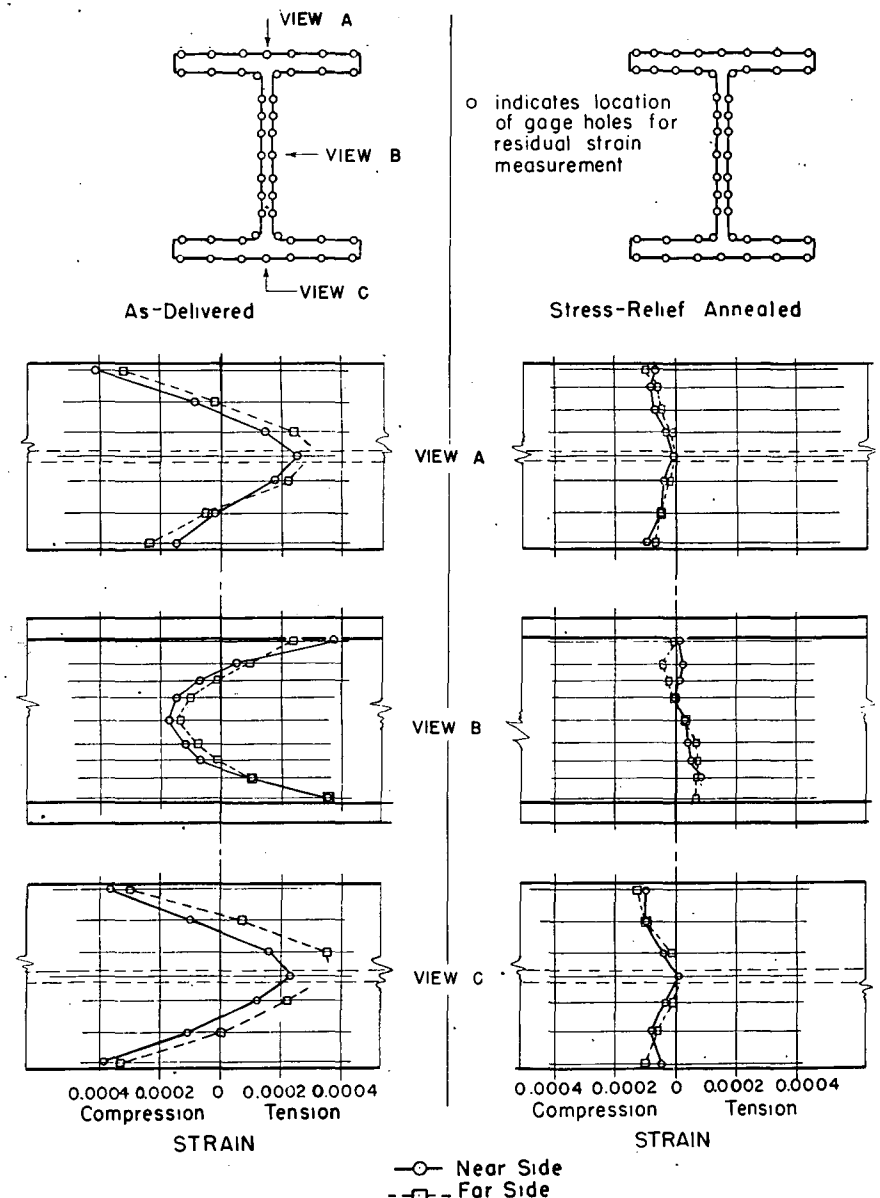

FIG.29 RESIDUAL STRAIN IN 8 WF67 BEAM

(a)

(b)

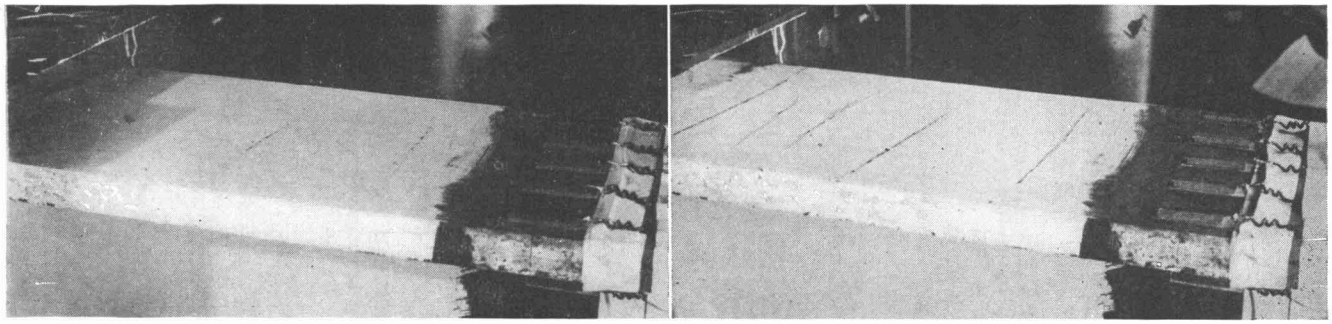

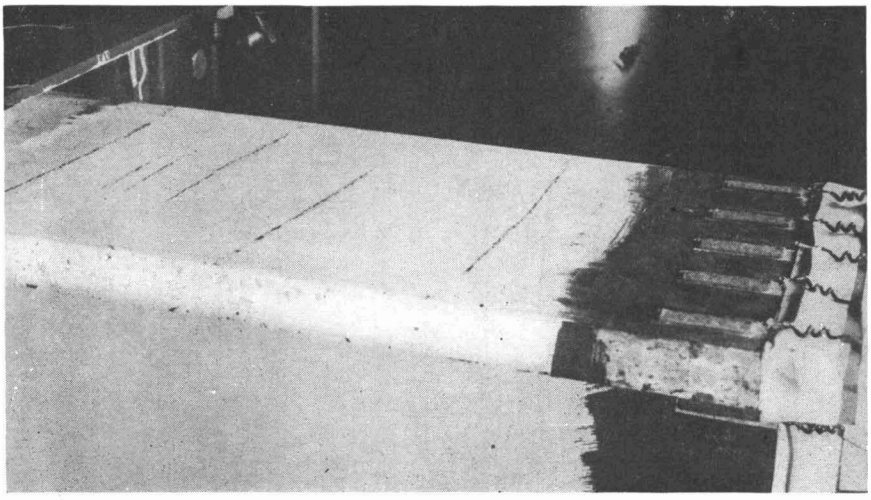

(c)

Fig. 30 (a) Test 4, 8WF67, annealed compression flange, after initial yielding at 94.3 kips.

Fig. 30 (b) Same view as Fig. 30 (a), after 1 hr. of yielding at 96.3 kips.

Fig. 30 (c) Same view as Fig. 30 (a), after several hours at 96.3 kips. Yielding had virtually stopped

the regular tests were loaded by web stiffeners as shown in Fig. 7.

Any or all of these factors might have contributed to the less-than-theoretical strength of the pilot tests, hence, no definite conclusion can be given from the foregoing comparison.

Test 1 may be compared with Test 2, the principal difference between the two being that Test 2 was annealed and Test 1 was not. As shown in Fig. 19, the agreement between Test 1 and the theoretical curve is good but, as previously discussed Test 1 consumed over a 2-wk. period and there are evidences of strain-aging at locations marked A to E on Fig. 19. Had Test 1 been run at the same speed as Test 2, the agreement with the theoretical probably would have been poorer.

Tests 3 and 4 in Fig. 20 may be compared on the basis that only one difference existed between the tests, that of residual stress levels. The strength of the as-delivered beam in Test 3 was definitely less than that predicted from the stress-strain data. As shown in Fig. 29 the residual stresses had maximum values of about 12 ksi. in both flanges and in the web of this beam.

The apparent effect of residual stresses in producing less-than-theoretical plastic moment capacity, in the case of Test 3, is largely discounted in practical importance by the fact that, in Test 4, in spite of the excellent theoretical agreement, the strength is nevertheless lower than the strength of the as-delivered beam of Test 3. This is due to the fact that the annealing generally lowered the yield strength of the material at the same time that it reduced the residual stresses.

The observed and calculated moments at initial yield, based on upper yield point, and after general yielding, influenced primarily by lower yield point, are presented in Table 2. Although the "observed" initial yield moment cannot be evaluated with much precision from the

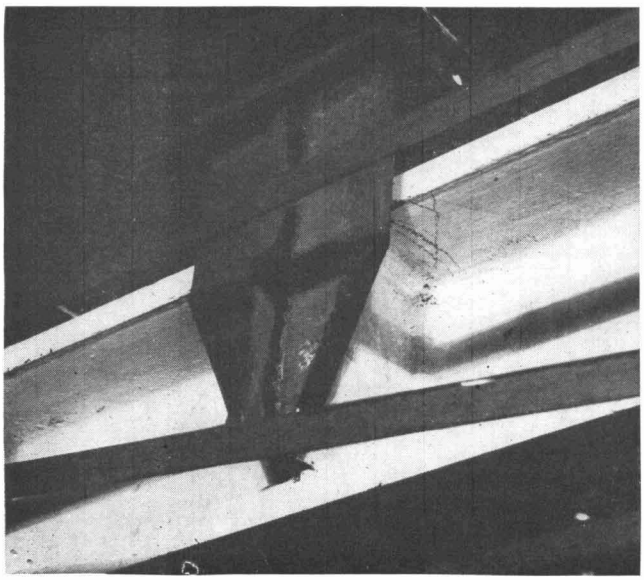

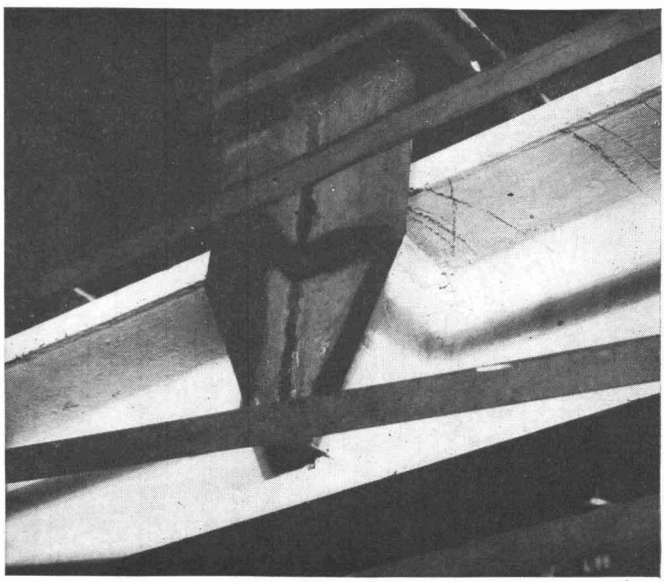

Fig. 31 (a) Test 4, underside of compression flange at load carrier, 96.3 kip load, after yielding had stopped

Fig. 31 (b) Test 4, same view as Fig. 31 (a), after 1 hr. of yielding at 98.3 kips.

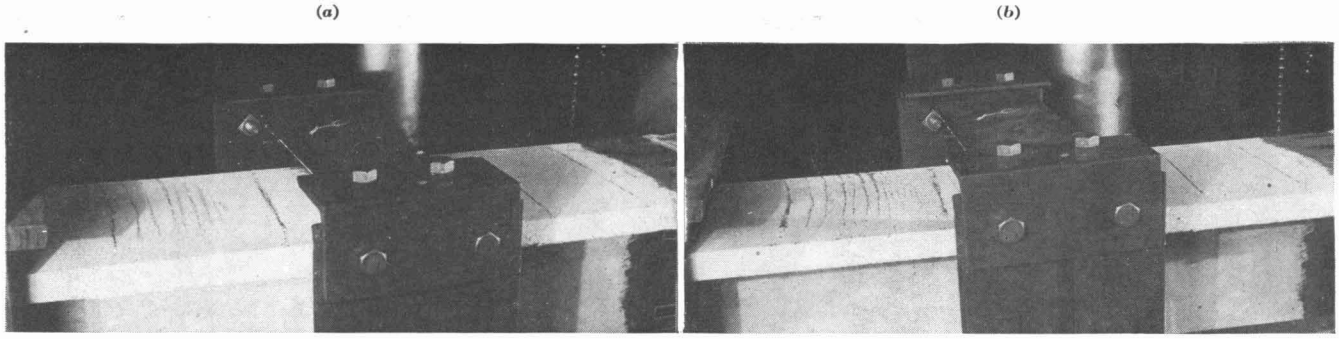

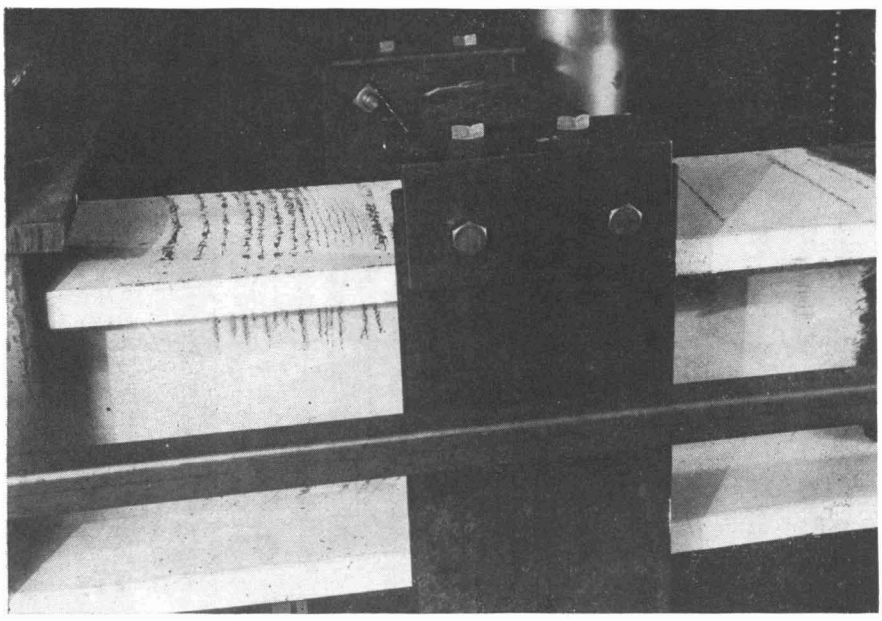

Fig. 32 (a) Test 4, top of compression flange after 1 hr. of yielding at 98.3 kips.

Fig. 32 (b) Test 4, same view as Fig. 32 (a), after 5 hrs. yield at 98.3 kips.

Fig. 32 (c) Test 4, same view as Fig. 32 (a), 1/2 hr. after applying maximum load of 100.3 kips.

M-ϕ curve, the agreement with the calculated value is good for the annealed beams. The "plastic moment," arbitrarily evaluated when the yielding had come within 2 in. of the neutral axis, was practically constant after this amount of yielding. The poorest agreement was in Test 3 of the as-delivered 8WF67, where the plastic moment determined by test was 93% of the calculated moment. In no case was the observed plastic moment appreciably greater than the calculated value.

As explained in the introduction, the theoretically calculated curves were based on the assumption that the upper yield point was maintained in the elastic region adjacent to the theoretical plastic boundary. However, in view of the small difference between the upper and lower yield points and therefore the inappreciable effect on the theoretically calculated M-ϕ curves, no conclusion on this question can be based on these test results. The fact that surface yield lines developed simultaneously on both surfaces of the upper flange would indicate that the upper yield point is not maintained after initial yielding, for, if it were, one would expect yielding to progress slowly from the outer to the inner surfaces of the flanges.

Another factor, that according to some investigators[7] might be expected to influence the test results, is a supposed increase in yield point attributed to a nonuniform elastic stress distribution. Others have disputed the foregoing proposition and have sought to demonstrate[4] that the phenomenon is primarily due to an unstable upper yield point which may be increased to an exaggerated degree under unusual conditions of smooth surface finish, precise loading, etc., obtained in specially machined specimens. Certainly the tests reported herein give no evidence of an appreciably increased strength due to nonuniform stress distribution or to any other cause and the question appears to be of academic interest.

The gradual spread of intermittent zones of yielding has been fully discussed under "test results."

Of importance to the calculation of ultimate or collapse strength of frames is the graphic illustration in Figs. 18 to 20 of the fact that the plastic moment or hinge moment of the beams was practically constant over a range of deflection and unit angle change, ϕ, of more than eight times the elastic range of the beams.

Some of the more important conclusions in the foregoing remarks are summarized as follows:

1. The M-ϕ curves for structural steel beams, laterally supported, can be predicted satisfactorily from the stress-strain tensile test curves and the usual theory of plastic bending based on the assumptions of uniform distribution of yield and strains pro-

Table 2—Summary of Test Results

Test No.	*Section*	*Internal stress condition*	*Initial yield moment, Kip-in.* *Calculated*	*Observed*	*Ratio: Obs. I.Y.M. / Calc. I.Y.M.*	*Plastic moment,* Kip-in.* *Calculated*	*Observed*	*Ratio: Obs. P. M. / Calc. P. M.*
Pilot-1	8WF31	As-delivered	1117	1012	0.91	1182	1145	0.97
Pilot-2	8WF40	As-delivered	1250	1037	0.83	1330	1260	0.95
1	8WF40	As-delivered	1301	1258	0.97	1430	1405	0.98
2	8WF40	Annealed	1255	1243	0.99	1366	1340	0.98
3	8WF67	As-delivered	2750	2285	0.83	3104	2900	0.93
4	8WF67	Annealed	2441	2585	1.06	2783	2780	1.00

* Arbitrarily taken as moment when yielded region had theoretically progressed to within 2 in. of neutral axis. The moment at this degree of yielding is near the maximum for no strain hardening.

(a)

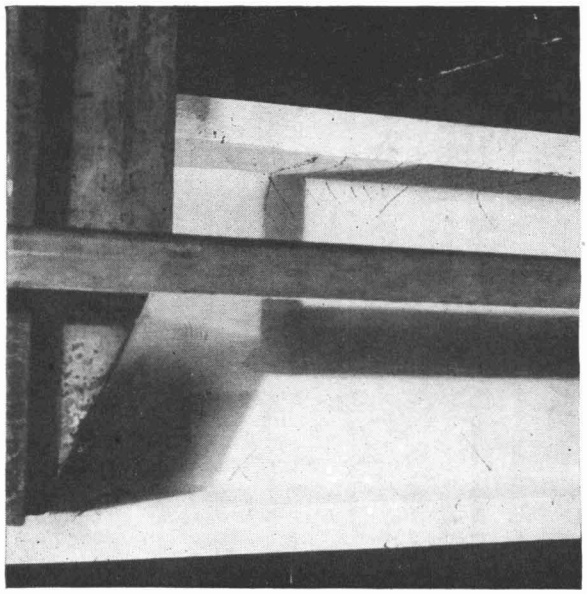

(b)

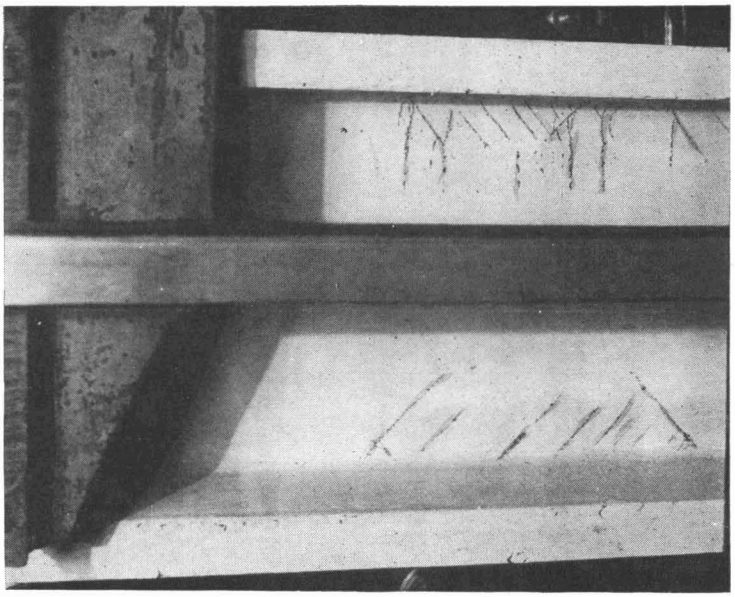

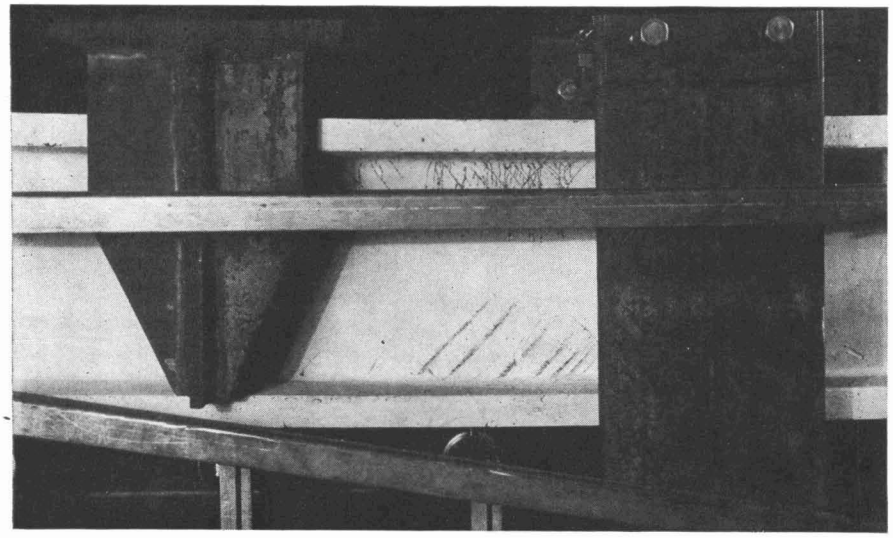

(c)

Fig. 33 (a) Test 4, side view after 1 hr. of yielding at 98.3 kips.
Fig. 33 (b) Test 4, same view as Fig. 33 (a) after 5 hr. yield at 98.3 kips.
Fig. 33 (c) Test 4, same view as Fig. 33 (a) 1/2 hr. after applying maximum load of 100.3 kips.

portionate to the distance from the neutral axis.

2. Agreement between experimental and theoretical M-ϕ curves, as calculated from the test coupon strength, was better for annealed beams than for as-welded beams.
3. Stress relief annealing causes a lowering of overall static bending strength.
4. The tests give no evidence of increased upper yield point or increased bending strength due to the nonuniform stress distribution in bending.

Appendix

CALCULATION OF *M*-ϕ CURVE

As stated in the Introduction, the calculated moment at initial yield of the beams was assumed as corresponding to the load at which the extreme fibers of the beam reached the upper yield point of the flange material. As shown diagrammatically by Fig. 41, the angle change per unit length, ϕ, is simply the maximum longitudinal strain divided by the distance from the neutral axis and may be expressed conveniently in terms of stress at the boundary of the elastic region of the beam.

M_1 and ϕ_1 at initial yield, therefore, are calculated to be:

$$M_1 = S\sigma_{UYF} \qquad (2)$$

$$\phi_1 = \frac{\epsilon_c}{c} = \frac{\sigma_{UYF}}{Ec} \qquad (3)$$

where

S = section modulus, in handbook
E = modulus of elasticity
ϵ_c = longitudinal strain at extreme fiber
c = distance from neutral axis to extreme fiber

The second pair of coupled M and ϕ values is most conveniently determined after yielding has progressed to the juncture of the fillets and the web, a distance y_2 from the neutral axis as shown in Fig. 1 (*b*). At this stage it is assumed that the region between the distances y_2 and c from the neutral axis are uniformly stressed to the lower yield point of the flange material, σ_{LYF}. The contribution of this region to the resisting moment is simply equal to the product of the stress times the static moment of the uniformly stressed area about the neutral axis. Then, after yielding reaches the web, the static moment of the plastic region equals that of the whole section less that of the rectangular web section that is still elastic.

Letting Z = static moment of whole section, $Z_2 = wy_2^2$ = static moment of the portion of the web having constant thickness. The contribution of the plastic portion to M_2 is $\sigma_{LYF}(Z - Z_2)$ and the contribution of the elastic portion is $\sigma_{UYW}I_2/y_2$ but $I_2 = \frac{2}{3}wy_2^3 = \frac{2}{3}Z_2y_2$. Hence the total resisting moment is

$$M_2 = \tfrac{2}{3}\sigma_{UYW}Z_2 + \sigma_{LYF}(Z - Z_2) \qquad (4)$$

and

$$\phi_2 = \frac{\sigma_{UYW}}{Ey_2} \qquad (5)$$

After yielding has progressed into the web to any distance y_3 from the neutral axis similarly computed M and ϕ values would be given by:

$$M_3 = \tfrac{2}{3}\sigma_{UYW}Z_3 + \sigma_{LYF}(Z - Z_2) + \sigma_{LYW}(Z_2 - Z_3) \qquad (6)$$

$$\phi_3 = \frac{\sigma_{UYW}}{Ey_3} \qquad (7)$$

The limit of M, as ϕ increases, and the whole section is assumed plastic, would be

$$M_4 = \sigma_{LYF}(Z - Z_2) + \sigma_{LYW}Z_2 \qquad (8)$$

Since most of the plastic strength of the section is realized as soon as the flanges have entirely yielded, the value of M_4 by Equation 8 is closely approached at ϕ values for which the maximum plastic strains are within the lower yield point

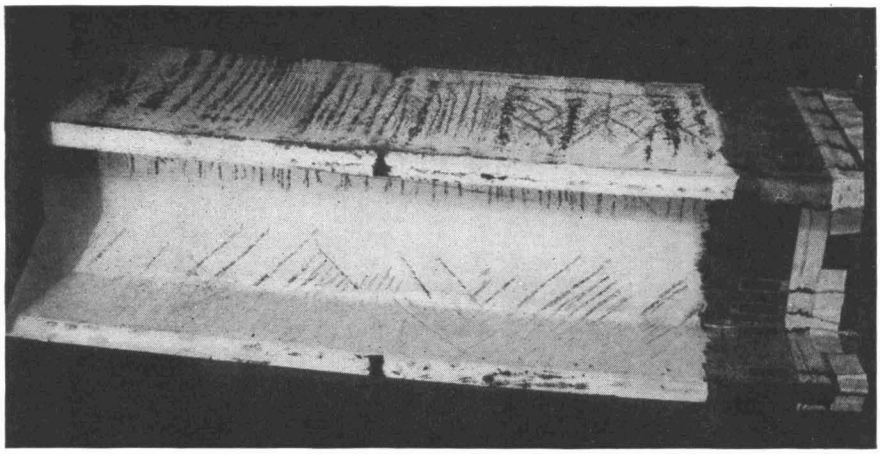

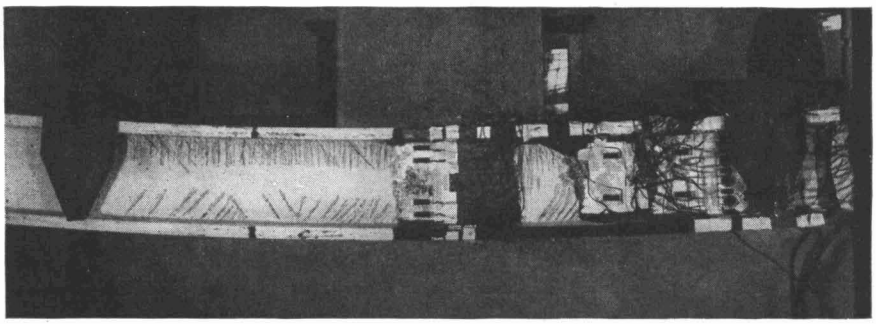

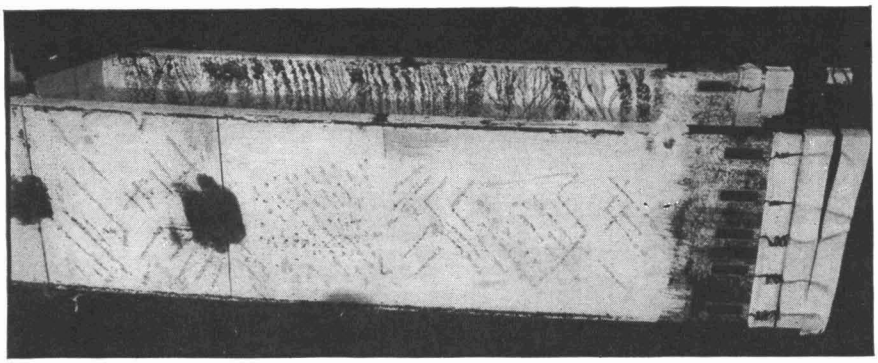

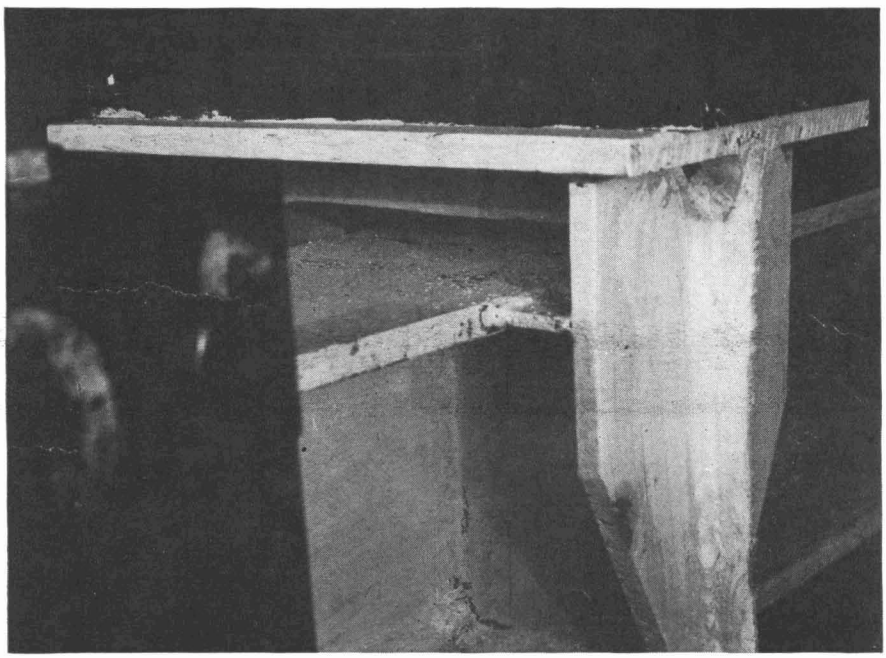

Fig. 37 Test 1, 8WF40 as-delivered, initial yield in compression flange at load carrier

Fig. 34 Test 4, after completion. Upper surface of top and bottom flange

Fig. 35 Test 4 after completion of test

Fig. 36 Test 4 after completion of test. Lower surface of top and bottom flanges

range prior to any general strain hardening. In the simply supported beam the deflections for usual span lengths will be far beyond permissible values before strain hardening commences in the outer fibers.

Equations 2 to 8 illustrate the procedure used in this report in obtaining theoretical M-ϕ curves. An illustrative example will now be given in which the procedure will be further simplified though slightly less accurate. Consider an 8WF67 section, for which the *A.I.S.C. Handbook* gives:

$S = 60.4$
$w = 0.575$, web thickness
$t = 0.933$, flange thickness
$b = 8.287$ in., flange width
$d = 9.00$ in., over-all depth

Assume both upper and lower yield points equal to the specification minimum of $\sigma_y = 33$ ksi. and assume $E = 30{,}000$ ksi. Neglect fillets, since these radii are not given in the handbook and the error will be about 1% on the safe side. Equations 2 to 8 for these assumptions, simplify to:

$$M_1 = 33S$$
$$M_2 = 33Z - 11Z_2$$
$$M_3 = 33Z - 11Z_3$$
$$M_4 = 33Z$$
$$\phi_1 = \frac{0.0011}{c}$$
$$\phi_2 = \frac{0.0011}{y_2}$$
$$\phi_3 = \frac{0.0011}{y_3}$$

Neglecting fillets, the static moments are given by

$$Z = bt(d - t) + \frac{w(d - 2t)^2}{4}$$

and

$$Z_2 = \frac{w(d - 2t)^2}{4}$$

$$Z_3 = 4w \text{ (assuming } y_3 = 2 \text{ in.)}$$

or, for the 8WF67

$$Z = (8.287)(0.933)(8.067) + \frac{(0.575)(7.134)^2}{4}$$

$$= (62.37)(7.32) = 69.69 \text{ in.}^3$$
$$Z_2 = 7.32 \text{ in.}^3$$
$$Z_3 = 3.73 \text{ in.}^3$$

Substituting these values in the expression for M and ϕ

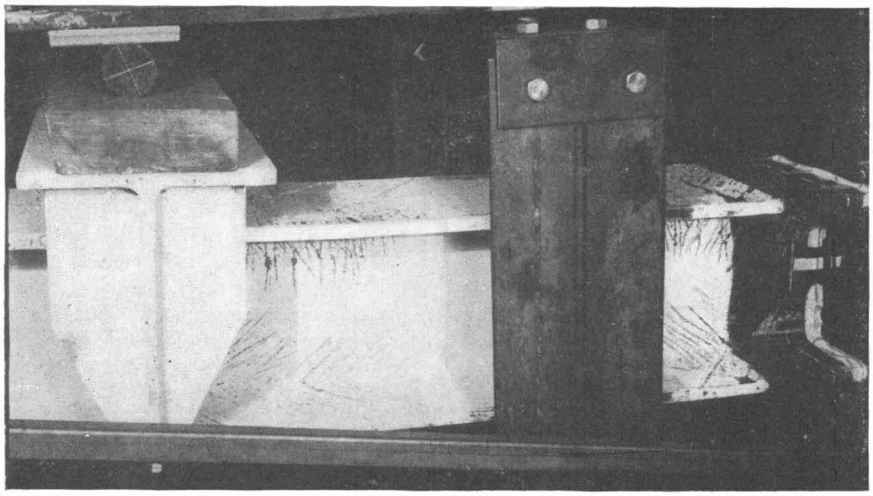

Fig. 38 Test 1 after completion of test

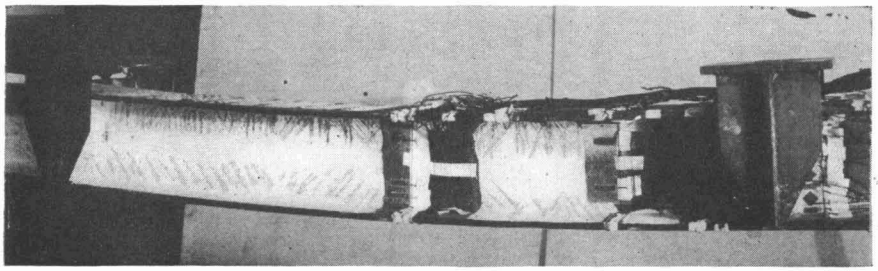

Fig. 39 Test 2, 8WF40, annealed, after completion of test

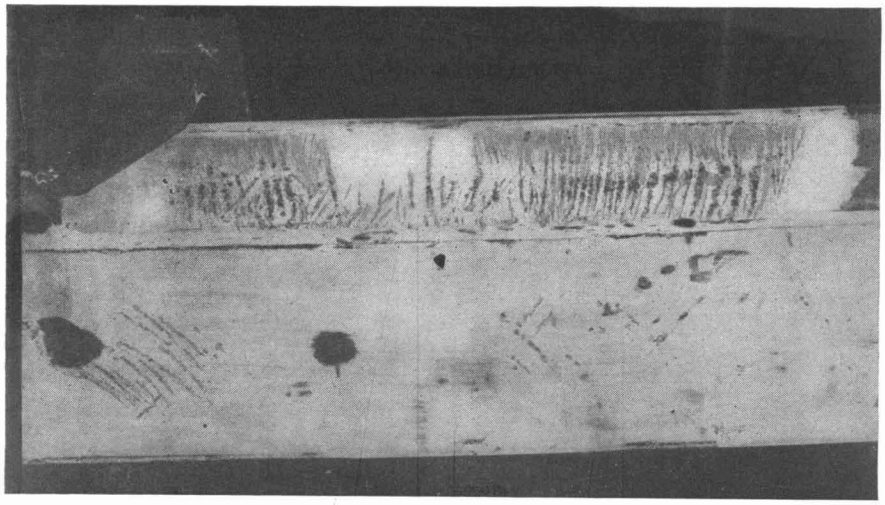

Fig. 40 Test 3, 8WF67, as-delivered, after completion of test

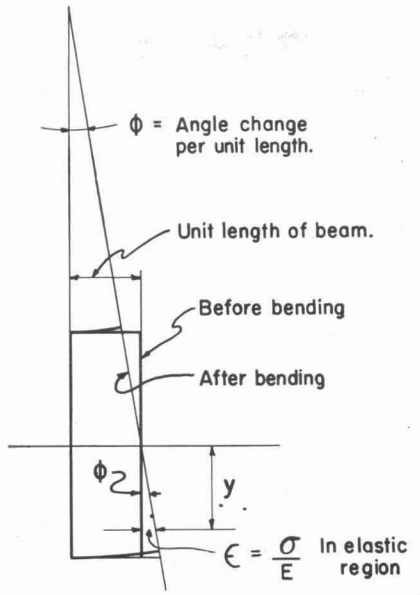

Fig. 41 Deformation of unit length of beam during bending

kip-in.	radians/in.
$M_1 = 1993.2$	$\phi_1 = 0.000244$
$M_2 = 2219.3$	$\phi_2 = 0.000308$
$M_3 = 2258.8$	$\phi_3 = 0.000550$
$M_4 = 2299.8$	

Figure 2 shows these calculated values and the curve that they define.

References

1. See any book on Strength of Materials; for example, Timoshenko, 2nd ed. Vol. 1, p. 134.
2. Nadai, A. *Plasticity*, McGraw-Hill, p. 160 (1931).
3. Timoshenko, S. *Strength of Materials*, Vol. 2, p. 362.
4. Morkovin, D., and Sidebottom, O., "The Effect of Non-Uniform Distribution of Stress on the Yield Strength of Steel," University of Illinois Experiment Station, Bull. No. 372 (1947).
5. Winter, G., "Strength of Thin Steel Compression Flanges," *Trans., Am. Soc. Civil Engrs.*, **112**, 527 (1947).
6. Madsen, I., "Box Girder Buckling Tests," *Iron Steel Engr.*, **18** (11), 95 (Nov. 1941).
7. Peterson, F. G. E., "Effect of Stress Distribution on Yield Points," *Trans. Am. Soc. Civil Engrs.*, 1201 (1947).